Cationic Cellulose Nanocrystals (CNCs) for Organic and Inorganic Colloids Flocculation

by

Xinyao Zhou

A thesis

presented to the University of Waterloo

in fulfillment of the

thesis requirements for the degree of

Master of Applied Science

In

Chemical Engineering

Waterloo, Ontario, Canada

AUTHOR'S DECLARATION

I hereby declare that I am the sole author of this thesis. This is a true copy of the thesis, including any required final revisions, as accepted by my examiners. I understand that my thesis may be made electronically available to the public.

Abstract

Cellulose nanocrystals were modified for use as novel flocculants by taking advantage of the extended cationic polymeric chains on CNCs. They were evaluated using both organic colloids and inorganic bentonite clay particles.

For the flocculation of organic colloids, cellulose nanocrystals (CNCs) were grafted with N-N-(dimethylamino) ethyl methacrylate (DMAEMA), 4-vinylpyridine (4VP) and polyamine. The amine-g-CNCs displayed the best flocculation performance from the lowest optimal mixing ratio at pH=4 and wider flocculation window at pH=7. Bridging effect was more obvious for P4VP yielding relatively large flocs. The presence of carbonyl group of PDMA polymer chains promoted hydrogen bonding that contributed to aggregate latex particle in alkaline condition.

For the inorganic clays, chitosan was utilized as natural polymer grafted onto CNCs. To enhance its water solubility, GTMAC were conjugated onto chitosan chains (G-chitosan) to produce the polymer flocculants. CNCs was firstly oxidized by sodium periodate to produce aldehyde groups, and G-Chitosan was grafted onto the aldehyde groups on CNCs to form novel polymer/nanoparticle, G-Chitosan/A-CNCs flocculants. For G-chitosan, the optimal dosages at pH 4 and 7 were 10 mg/L and 50 mg/L respectively. For the G-Chitosan/A-CNCs, the OD was 10 mg/L, 50 mg/L and 177 mg/L at pH 4, 7 and 10, respectively. The impact of the polymer was less significant when it was associated with CNCs particle. The role of CNCs in flocculants was related to its high aspect ratio and hydrophobic stiff backbone. Flocs parameters, such as size, shape and fractal dimension were further used to elucidate the significant of incorporating CNCs to the flocculants.

Acknowledgements

I would like to express my deepest gratitude to my supervisor, Professor Michael K. C. Tam for providing me a chance to explore research on flocculation and his constant support in the Laboratory for Functional Colloids and Sustainable Nanomaterial. I am thankful to have this chance of being trained under Dr. Tam's kind supervision.

I would also like to thank members of my committee Prof. Boxin Zhao and Prof. Shirley Tang for their insightful comments and constructive criticism. Their guidance helped to strengthen the quality of this thesis.

I would also like to extend my sincere gratitude to Dr. Jeuwen Liu for granting me access to his equipment that provides a better characterization of my research. Floc size, morphology and zeta potential analysis were determined using Malvern Nano ZS Zetasizer DLS system and Microscopy instrument respectively.

Special thanks are due to all of my lab mates, Dr. Shi who taught me about polymerization, Reynard always inspired me for many new ideas and insightful suggestions; Nate for constantly helping me in all lab activity and always patient with me during my difficulties.

Especially thanks to Nate, Abel and Rachel for editing my draft paper, I appreciate their labor and work.

I would like to take this opportunity to thank my mother for her continual love, and encouragement in my life.

My husband Kai, is my best companion in every situation, I am deeply contented to have him as my family, my friend, my teacher and my counselor.

As a Christian, I would like to praise the Lord my God, in Colossians 1:16 of the Bible, it reads "Because in Him all things were created, in the heaven and on the earth, the visible and the invisible, whether thrones or lordships or rules or authorities, all things have been created through Him and unto Him."

Table of Contents

AUTHOR'S DECLARATION ..... **ii**

Abstract ..... **iii**

Acknowledgements ..... **iv**

List of Figures ..... **ix**

List of Tables ..... **xii**

List of Schemes ..... **xiii**

Chapter 1. An review on the Flocculation-Coagulation in Wastewater Treatment: Multifarious Coagulants/Flocculants **1**

1.1 Background of wastewater, characterization and treatment processes **1**

1.2 Categories of multifarious coagulants/flocculants **3**

1.3 Inorganic coagulants **4**

1.4 Synthetic organic flocculants **7**

1.4.1 Various types of polymers 7

1.4.2 Cationic polyelectrolytes and applications 8

1.4.2 Anionic polyelectrolytes and applications 11

1.4.3 Non-ionic and amphoteric polyelectrolytes and applications 12

1.4.4 Factors that impact flocculation of synthetic organic flocculants 16

1.5 Polymer grafted bio-flocculants **17**

1.5.1 Chitosan....18

1.5.2 Cellulose....20

1.5.3 Starch....23

1.6 Summary and discussion....25

Chapter 2. Cationic Cellulose Nanocrystals (CNCs) for Organic Colloidal Latex Particle Flocculation....29

2.1 Introduction....29

2.2 Experiment....31

2.2.1 Materials and Instrumentation....31

2.2.2 Sample synthesis....32

2.2.3 Characterization....33

2.2.4 Flocculation experiments....34

2.3 Results and Discussion....36

2.3.1 Characterizations of polymer grafted CNCs....36

2.3.2 Flocculation performance....39

2.4 Conclusions....50

Chapter 3. GTMAC-Chitosan Modified Cellulose Nanocrystals (CNCs), a Novel Polymer/Nanoparticle Flocculants for Bentonite Clay Flocculation....51

3.1 Introduction....51

3.2.1Materials....54

3.2.3 Periodate oxidation of CNCs 55

3.2.4 Preparation of GTMAC-Chitosan modified Aldehyde-CNCs 56

3.2.6 Flocculation experiments 58

3.3. Results and discussion.....59

3.3.1 Flocculants characterization.....59

3.3.2 Evaluation of the optimal dosage of the flocculants at various pH levels 65

3.3.3 Floc size: Projected area diameter D (μm).....70

3.3.4 Flocs shape and fractal dimension 72

3.4 Comparison between GTMAC-Chitosan and G-Chitosan/A-CNCs.....78

3.5 Conclusions 80

Chapter 4. Conclusions and Recommendation for Future Studies 82

Reference.....85

List of Figures

Figure 1.1 Classification of coagulants/flocculants. 4

Figure 1.2 Coagulation-flocculation of the commercial CPAM and DCC assisted with $CaCl_2$ with the effluent before and after coagulation-flocculation: (a) turbidity, COD_{Cr} and BOD_5 of the suspensions (c) BPC-g-PAM and PAM treated with the effluent from paper mill (d) BPC-g-PAM and commercial PAM treated with standard kaolin suspension, (b), (d), (f) digital photographs of the suspensions before and after coagulation-flocculation treatment. 22

Figure 2.1 FT-IR spectra of CNCs, PDMA-g-CNCs, P4VP-g-CNCs and amine-g-CNCs. 37

Figure 2.2 Conductometric titrations of (a) PDMA-g-CNCs, (b) P4VP-g-CNCs, (c) amine-g-CNCs and (d) carboxylic acid latex with sodium hydroxide. 37

Figure 2.3 Zeta potential value of PDMA-g-CNCs, P4VP-g-CNCs, amine-g-CNCs and carboxylic acid latex samples. 38

Figure 2.4 Summary of different types and amounts of functional group both in cationic CNCs and anionic latex. 39

Figure 2.5 Calibration curve of solid content with transmittance under pH 4, 7 and 10. 40

Figure 2.6 Flocculation efficiency of PDMA-g-CNCs with latex suspension with various mixing ratio under three different pHs (a) Digital pictures of sample after flocculation and 24h; (b) flocculation efficiency results calculated from UV-vis transmittance. 41

Figure 2.7 Flocculation efficiency of P4VP-g-CNCs with latex suspension with various

mixing ratio under three different pHs (a) Digital pictures of sample after flocculation and 24h; (b) flocculation efficiency results calculated from UV-vis transmittance.....43

Figure 2.8 Flocculation efficiency of Amine-g-CNCs with latex suspension with various mixing ratio under three different pHs (a) Digital pictures of sample after flocculation and 24h; (b) Flocculation efficiency results calculated from UV-vis transmittance.....44

Figure 2.9 Floc properties under three different pHs from PDMA-g-CNCs flocculants (a) Zeta potential value and (b) Floc size.....45

Figure 2.10 Floc properties under three different pHs from P4VP-g-CNCs flocculants (a) Zeta potential value (b) floc size. 47

Figure 2.11 Floc properties under three different pHs from Amine-g-CNCs flocculants (a) Zeta potential value (b) floc size. 48

Figure 3.1 FT-IR spectra of CNCs, A-CNCs. 60

Figure 3.2 Conductomatric titration of (a) GTMAC-Chitosan and (b) Dicarboxylic acid CNCs. 61

Figure 3.3 GTMAC-Chitosan/A-CNCs flocculants (a) solubility; (b) particle size. 62

Figure 3.4 Flocculation characteristics of three different bulk clay concentrations with varied flocculants dosage (mg/L) (a) GTMA-Chitosan; (b) G-Chitosan-g-A-CNCs 63

Figure 3.5 TEM image of (a) pristine CNCs (b) G-Chitosan/A-CNCs. 64

Figure 3.6 ξ-potential value of bentonite clay, G-Chitosan and G-Chitosan/A-CNCs flocculants over pH range from 3 to 11.....65

Figure 3.7 Residual turbidity and ZP by adding G-Chitosan and G-Chitosan/A-CNCs, respectively as a function of dosage (mg/L) under pH 4, 7 and 10 respectively: (a), (b) and (c) are the G-Chitosan sample; (e), (f) and (g) are the G-Chitosan/A-CNCs sample. 69

Figure 3.8 Projected area diameter of floc as a function of flocculants dosage (mg/L) (a) G-Chitosan; (b) G-Chitosan/A-CNCs. 71

Figure 3.9 Microscopy image of floc under varied dosage of G-Chitosan a) pH 4, b) pH 7 and c) pH 10, OP has been marked out as red frame. 74

Figure 3.10 Shape factor with varied GTMAC-Chitosan dosage under pH 4, 7 and 10 74

Figure 3.11 Microscopy image of floc under varied dosage of G-Chitosan/A-CNCs a) pH 4, b) pH 7 and c) pH 10, OP has been marked out as red frame.....76

Figure 3.12 Shape factor with varied G-Chitosan/A-CNCs dosage under pH 4, 7 and 10.....76

List of Tables

Table 1.1 The molecular weight properties of synthetic organic flocculants.....8

Table 1.2 Synthetic cationic polymer flocculants, applications and optimal results.....10

Table 1.3 Synthetic anionic polymer flocculants, applications and optimal results 12

Table 1.4 Synthetic anionic polymer flocculants, applications and optimal results 14

Table 1.5 Types of starch-based bio-flocculants applications and optimal results 25

Table 1.6 Summary of advantages and defects of various coagulants/flocculants 26

Table 2.1 The optimal dosage and corresponding flocculation efficiency of cationic flocculants. 49

Table 3.1 The optimal dosages and corresponding dimension fractal parameter D_2 77

List of Schemes

Scheme 1.1 Factors that impact flocculation of synthetic organic flocculants.....17

Scheme 1.2 Synthesis of ampholytic/cationic cellulose as bio-flocculants.....23

Scheme 2.2 Synthesis of PDMA-*g*-CNCs, P4VP-*g*-CNCs and amine-CNCs.....33

Scheme 3.1 Synthesis of GTMAC functionalized chitosan. 55

Scheme 3.2 Periodate oxidation of CNCs. 56

Chapter 1. An review on the Flocculation-Coagulation in Wastewater Treatment: Multifarious Coagulants/Flocculants

1.1 Background of wastewater, characterization and treatment processes

Ensuring safe and clean water is an admirable goal for many nations through the world but especially those facing the clean water shortage resulting from high rate of industrial and personal consumption. Today, much is known about the safety of drinking water and how they relate to human health. Waterborne health hazards include biological agents (pathogenic bacterial, viruses, and parasites), chemical agents and radioactive pollutants.[1]

One of the most important physical characteristics is solid content, the operational definition of total solids (TS) are categorized by size of total suspended solids (TSS), which include settable (>100μm) and non-settable (1nm-100μm), and dissolved solid (DS) (<1nm).[2] Wastewater normally contains thousands of different organic species, which are denoted as biochemical oxygen demand (BOD), chemical oxygen demand (COD) or total oxygen demand (TOD) by calculating the depletion of dissolved oxygen within the water sample. Non-organic contaminants may be quantified by nitrogen and phosphorous oxidation.[3–5] Chemically involved contaminants are persistent organic pollutants, such as polychlorinated biphenyls, dichlorodiphenyltrichloroethane (DDT), and emerging pollutants,[3][6] for instance, pharmaceuticals and personal care products. Biological test on wastewater are used to assess whether pathogenic organisms such as bacteria, virus, germ or protozoa within the safety limits for drinking, swimming or discharge into the

environment.

The main subjects of conventional wastewater treatment processes are reduction of BOD, COD, TSS followed by disinfection before discharge.[7] In order to achieve the desired water quality, multiple treatment processes are combined in series, such as pretreatment, primary treatment, secondary treatment, tertiary treatment and sludge disposal. Pretreatment and primary treatment are generally used to screen coarse solids and colloidal particles, the secondary biological process such as coagulation-flocculation, flotation and sedimentation and filtration are used to remove organic matter through biochemical oxidation.[8] Waste may be pretreated anaerobically to allow microorganisms to settle, then organics may be removed by treatment, such as adsorption, stripping, and biodegradation.[9–11]

Coagulation-flocculation process was found to be cost effective, easy to operate and less energy required than other alternative treatment approaches. Since the 19th century, Fuller published his work in the United State on the development of a rapid sand filter using aluminum sulfate, which resulted in rapid use of coagulation-flocculation in industrial applications.[12] Flocculation is a well-established process in transforming small particles into larger aggregates; coagulation describes subsequent process whereby the destabilized colloids in the micro or sub-micro size range undergo further aggregates growth.[13] Coagulation-flocculation process has proven to be advantageous in the pre-treatment and primary treatment phases in solid-liquid separation processes, which reduces membrane fouling and is very compatible with other upstream or downstream treatment processes to enhance the working efficiency of the combined unit.

1.2 Categories of multifarious coagulants/flocculants

The aim of coagulation-flocculation (CF) treatment is primarily to remove colloidal matter present in the wastewater. Recently, CF technology exhibits great potential in various applications, such as heavy mental adsorption,[14–17] microalgae harvesting,[18–21] and removal of dye [22–28] and organic matter.[29–36] Colloidal particles are well-known for high adsorption and long-term stability, by virtues of their nanometer-size and large specific surface area.[37] Their charged surfaces enable them to repel each other and allow for their high mobility in solution. The basic principle of coagulation is combining small particles into large aggregates so that the impurities can be removed by subsequent solid-liquid separation.[13] Upon the addition of flocculants, the destabilized small aggregates can be brought together to form macro flocs. When the flocs grow large enough, the effects of gravity become significant enough to overcome the hydrodynamic shear force, resulting in the precipitation from solution.[38]

Coagulant and flocculants can be classified into four categories, which are metals salts,[14,20,21,30,33,36,39–41] synthetic organic polymer,[40,42–53] and polymer-grafted bio-flocculants,[54–62] as shown in Figure 1.1. In the case of inorganic coagulants, both monomeric and polymeric salt have been used. Furthermore, the polymeric salt can either complex with inorganic moieties, such as silicate,[63–65] zinc[63], or organic polymer to form inorganic/organic hybrid.[28,66–68]

Organic polymer flocculants are mainly petroleum-based synthetic polymer. The intrinsic cationic functional group and polymer structure play an essential role in the flocculation process. The addition of polymer flocculants could accelerate the formation of mircoflocs by charge

attraction and neutralization, and the large flocs are allowed to settle and separate from the effluent stream.[69]

Recently, bio-flocculants have attracted increasing attention due to the concern of environmental effect and health risks from inorganic and organic coagulants. Therefore, more sustainable alternatives, such as polyelectrolyte grafted natural polymer including cellulose,[70–72] chitin,[73,74]chitosan,[75–78] starch[79–82] have been utilized. Through grafting approach, the polymer content has been greatly reduced in order to achieve comparable flocculation efficiency.

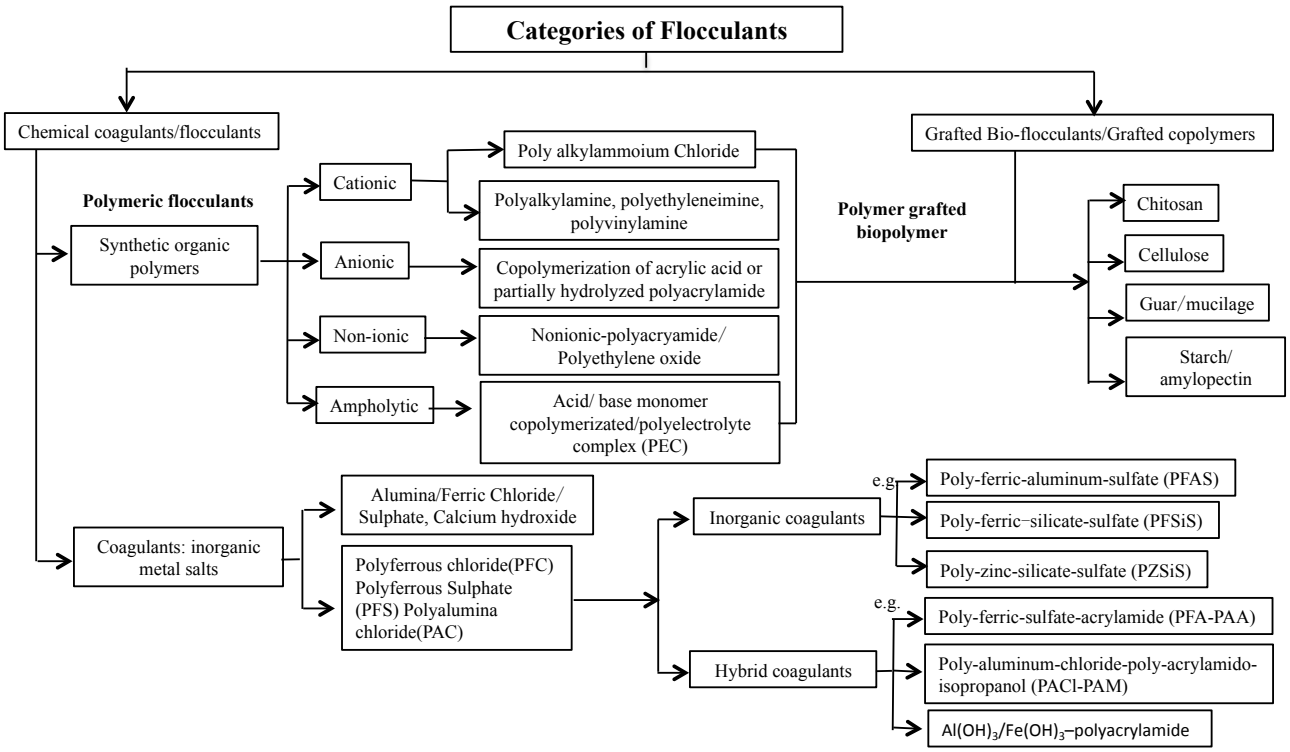

Figure 1.1 Classification of coagulants/flocculants.

1.3 Inorganic coagulants

Nearly all colloidal impurities in aqueous medium carry negative charges, covered by a hydration shell surrounded with counter-ions. As a result, they are very stable and highly mobilized due to

electrostatic repulsive forces. Coagulants of inorganic metal salts that were extensively used for the coagulation-flocculation of suspended particles are Al/Fe (III) salts. In neutral pH, the hydrolysis of metal salt will produce a large quantity of cations in suspension, which will adsorb onto the suspended particle surface, compress the colloid electrical double layer and neutralize the charge. These adsorbed cations will continue to hydrolyze into metal hydroxide, which renders the particle surface to be hydrophobic. The synergistic effects from charge neutralization and metal hydroxides precipitation promote the particle aggregation and floc propagation.

Many factors including wastewater composition, pH, coagulants type and dosage played an important role in the coagulation-flocculation efficiency. Guo et al. reported on the removal efficiencies of various hazardous A_s and S_b species using ferric salt in the following orders; As(V)>Sb(III)>As(III)>Sb(V). It was found that ferric sulphate was more favourable in removing antimony ions.[14] A_s(III) removal depended more on the coagulant dose and the number of sites available on the hydroxide surfaces, however, A_s(V) removal efficiency was related to the zeta potential of the colloidal suspension, therefore it was influenced more compared to As(III).[30] It was showed by Sanyano and coworkers that aluminum and ferric coagulants required lower dosage in neutral pH condition compared to pH of 10 in algae harvesting due to the fact that pH can affect cations hydrolysis route and change their existing form.

Conventional coagulation process has a serious problem as it is extremely rapid and uncontrollable, resulting in rapid precipitation.[83] In order to overcome this drawback, one successful approach is to partially hydrolyze inorganic coagulant prior to their addition to raw water

to maintain the desired species. The most popular polynuclear hydrolysis products are $Al_{13}O_4(OH)_{24}^{7+}$ or "Al_{13}".[84] They are kinetically stable and their thermodynamic equilibrium state can be controlled by the preparation conditions. A series of coagulant systems, such as poly alumiunium chloride (PAC),[64] poly ferric sulfate (PFS),[63] poly ferric chloride (PFC)[85] have been prepared using this approach.

Inorganic incorporated polymeric coagulants, such as metal-polysilicate complexes mainly contain Al-polysilicate or Fe-polysilicate, and they complex positively charged metal-coagulant and negatively charged polysilicic acid (PS). The effect of mixing ratio between Al/Si, Fe/Si, Si/Zn has been studied, for example, by varying the ratio and reaction time, a new type of iron-based polymer, poly-silicic-ferric produced different coagulants morphology either in chain-like or mutli-branched structure.[63] Studies on the hydrolysis-polymerization process of aluminum (III) with polysilicic acid have shown that the complexes with oppositely charged species possessed a lower net charge but a larger molecular weight, which indicates that both aggregating efficiency and charge effectiveness need to be taken into consideration.[63][86] Chen et al. systematically investigated the effects of Zi/Si ratio, with the addition of zinc, which can prevent the gelation of poly-silicic acid (PSA), thereby enhancing the stability and improving the charge neutralization capability.[87]

The composite of inorganic-organic compounds coagulants/flocculants also have been advanced. High molecular weight molecular polymer, polyacrylamide (PAM), associated with a varieties of inorganic coagulants such as $Al(OH)_3$ [68][28], $FeCl_3$,[88] $Fe(OH)_3$[89], $CaCl_2$[90], $MgCl_2$[91][92], $Mg(OH)_2$[93], are among the common polymeric hybrid coagulants/flocculants. Sun et al.

discovered that the star-like morphology could strengthen the interaction and adhesion between $Al(OH)_3$-PAM to solid surfaces to produce pellet-like floccules by applying single molecular force spectroscopy.[66] Furthermore, inorganic pre-polymerized iron-based coagulant polyferric sulphate (PFS) with a non-ionic polymer (polyacrylamide) hybrid under varied PAA/Fe (mg/L) and OH/Fe molar ratio, has been systematically investigated, such as the effective polymer species concentration and long term stability and good bridge mechanism.[29]

1.4 Synthetic organic flocculants

1.4.1 Various types of polymers

The development of organic polymers has advanced in many areas of application, such as oil-contaminated refinery sludge,[94] ceramic waste,[95] domestic waste disposal, [96] polymer manufacturing plant effluent,[97] tannery wastewater,[98] microalgae harvest,[19,42,99,100] and dye-contaminated water in recent years.[48,101] Their remarkable abilities to flocculate sols even in small quantities make them promising coagulant aids. In most cases, the synthetic organic flocculants are petroleum-based and non-renewable materials.

The characteristics of polymer charge and molecular weight are summarized in Table 1.1.[102] Organic flocculants can be characterized according to the nature of the ionic group present on the polymer chain, such as cationic, anionic, nonionic and amphoteric. The nature of the charge and charge density, molecular weight and conformation are the main factors that dominate the flocculation characteristics.

Table 1.1 The molecular weight properties of synthetic organic flocculants

Natural of charge	Cationic / Anionic / Nonionc / Amphoteric	
Molecular Weight	Low	1-3 millions
	Medium	3-6 millions
	Standard	6-10 millions
	High	10-15 millions
	Very high	Greater than 15 millions

1.4.2 Cationic polyelectrolytes and applications

Table 1.2 summarizes the various applications of cationic flocculants and the role of synthetic organic flocculants. Cationic flocculants are described by the ionizable groups of the monomeric units, such as amide,[45][103] quaternary ammonium salts (cryloxyethyltrimethyl ammonium chloride (DAC),[104,105]methacryloxyethyltrimethyl ammonium chloride (DMC),[105,106] dimethyldiallyammonium chloride (DMDAAC),[105] and functional amines. The effectiveness of various types of flocculants is commonly evaluated by turbidity, TSS, TOD, BOD and nitrogen/phosphorus removal. For example, cationic PAM is an important flocculant with medium to high molecular weight, which shows good performance at a low dosage of 5 mg/L for the removal of phytoplankton community without cell damage.[107] High molecular weight of C-PAM was found to require lower dosage to reduce membrane fouling compared with anionic and neutral polymer.[108]

Counterions effect has been investigated in terms of flocculation behavior of cationic polymer polydiallyldimethylammonium chloride (PDADMAC). Atomic force microscopy (AFM) showed that $PDADMANO_3$ adopted a flat and layer-by-layer adsorption, while $PDADMASO_4$ had “loops and tails” on the particle surface resulting in a bridging action, which explained that NO_3^-

counterion has a stronger flocculation efficiency and SO_4^- has a wider optimum dosage.[109] Lee et al. showed that polyamine synthesized by polycondensation of dimethylamine (DMA) and epichlorohydrin (EPI) could improve the removal efficiency and reduce 50% of PAC consumption in wastewater pilot plant.

Copolymerization could provide a synergistic effect in the cases of grafting quaternary ammonium group containing polymer (such as cryloxyethyltrimethyl ammonium chloride (DAC),[104] methacryloxyethyltrimethyl ammonium chloride (DMC),[110] dimethyldiallyammonium chloride (DMDAAC)[111] onto PAM via copolymerization. A certain amount of acrylamide in the polymeric flocculants used in water treatment can be limited by substituting it with an isomeric monomer — N-vinylformamide (NVF) that is nontoxic and very reactive in homopolymerization as well as copolymerization reactions. The presented results confirmed that acrylamide cationic copolymers with diallyldimethylammoniumchloride or terpolymers containing N-vinylformamide can be applied for the effective flocculation of mineral suspensions, such as fine coal and talc, sewage turbidity[112] and precipitate calcium carbonate (PCC).[104]

Table 1.2 Synthetic cationic polymer flocculants, applications and optimal results

Categories	Polymer	Chemical structure/funtional group	Molecular weight	Application	Optimum result	Refs.
Cationic	C-polyacryamide (PAM)	Amide	medium to high 100 to 500 kDa and	Phytoplankton community5 mg/l. dissolved organic carbon (DOC)	3 mg/l, removal ability (80%) 1 mg/L with 15 mg/ L PACl turbidity >60%,	Jancula et al. (2011) Wang et al. (2013)
	polydiallyldimethylammonium chloride (PDAMAC)	Quaternary amine	$4.8X10^3$	kaolin suspended solution, 1g/L	0.5 mg/L,pH 7.53,turbidity removal (98%)	Tian et al. (2007)
	polyamine	Amine	$1.0x10^4$-$5.0x10^4$	Industry waste	1.0 mg/L, Turbidity 88%, TOC 34% removal	Lee et al. (2001)
	polyacrylamide-c-methyl acrylate (PAM-c-MA)	Amide	$6x10^6$	industry waste, Turbidity, TSS, COD, Chromium	5mg/Lwith 100mg/L Al(SO4)2, Turbidity 97%, TSS 93.5%, COD 36.2%, Chromium 98.4% remove	Haydar & Aziz (2009)
	Polyacrylamide-quaternised aminoalkylacrylate (PAM-c-AMA)	Quaternary amine	$2\text{-}6x10^6$	celestite	pH 7, 0.02mg/L, 40% turbidity remove	Ozka & Yekeler (2004)
	pAAm/N-vinylformamide (NVF)/DADMAC		N-M	fine coal, colloidal silica and talc	3.0 mg/L, colloidal silica, 93%, fine coal 68%, talc 34	Ubowska et al. (2010)
	Polydimethyl aminoethane methacrylate	Amine	$3.9X10^4$ to $1.2x10^6$	domestic waste, TSS, COD, Turbidity	0.1 mg/L, with Ca (OH)2 250 mg/L, COD 48% remove, TSS 82% remove	Velásquez et al. (1998)
	poly 2-vinyl pyridine	Pyridine			4 mg/L, with Ca (OH)2 250 mg/L, COD 40% remove, TSS 80% remove	
	polyacryamide -c-poly acryloxyethyltrimethyl ammonium chloride (PAM-c-DAC)	Quaternary amine	branched	sewage turbidity, COD	20 mg/L, turbidity 87.67% remove, COD 57% remove	Sun et al. (2013)
			N-M	percipetate calcium carbonate (PCC)	20 and 4mg of copolymer/g of PCC in distilled water (pH 5.9) and industry water (pH 7.8)	Lam et al. (2014)

1.4.2 Anionic polyelectrolytes and applications

Partially hydrolyzed polyacrylamide with a number of acrylic units along the main chain is called A-PAM. The effects of A-PAM conformation were investigated by Cengiz et al. (2009) and Eyup et al. (2012) in processing ceramic waste and removing travertine, respectively.[113,114] They discovered that anionic unique molecular architecture (UMA) of A-PAM promoted more chain interaction and offered optimum flocs settling rate and lower residual. Polyacrylic acid (PAA) is another important anionic polyelectrolyte. Scott et al. (1996) [115] established relationships between polymer viscosity and flocculants activity, under controlled agitation. The results showed that higher molecular weights do improve flocculation performance on a per-molecule basis. By comparing the flocculation behaviour between the polyacid of high molecular weight (the reference) and the mixture of the other two polyacids, Yan et al. (2004) [116] observed that the presence of a relatively small amounts of a short-chain in the mixture greatly improved floc shear resistance compared to the case of a single-component high molecular weight polyacid. Rather than more toxic C-PAM, PAM-MAA under similar condition could reduce the usage of $Al_2(SO_4)_3$ which lower the chemical cost per cubic meter of wastewater treatment by almost 50%.[50] Novel thermal-responsive co-polymer, poly N-isopropyl acrylamide (PNIPAM)-co-AA is able to serve as a flocculants, collector as well as a dispersant below the lower critical solution temperature (LCST). Increasing the temperature above LCST, the polymer rapidly becomes hydrophobic and self-aggregates, recovering the valuable mineral through unselective particle entrapment into hydrophobic flocs.[52]

Table 1.3 Synthetic anionic polymer flocculants, applications and optimal results

Categories	Polymer	Funtional group	Molecular weight	Application	Optimum result	Refs.
Anionic	A-PAM	Acrylic acid	N-M	polymer manufacturing plant effluent, COD, SS	7.5mg/L of $Al_2(SO_4)_3$, COD, SS 90% remove	Sher et al. (2013)
			$14x10^6$	ceramic waste, 27 g/L	55.5 g/ton, pH 8.71, 96% remove	Cengiz et al .(2009)
			$5x10^6$	effluent treatment	pH 6 and 8, 7.5 ml/L COD, SS and turbidity up to 98%, 91% and 99% remove	Sher et al. (2013)
			1700	bentonite, calcium fluoride	10mg/L, turbidity and calcium fluoride remove >95%	Ponou et al. (2014)
	poly(acrylic acid) (PAA)		$2.5x10^5/1x10^6$	alumina particles, 25g/L	46 ppm for lower one, 83 for higehr one, neutral pH	Yan et al. (2004)
	polyacryamide-c-polymethylacrylic acid (PAM-c-MAA)		$1.5x10^7$	tannery wastewater	5 mg/L with 100 mg/L Al2(SO4)3, 96.3% for TSS, 48.3% for TCOD, 99.7% for chromium	Haydar et al. (2009)
	polyacryamide-c-polyacrylic acid (PAM-c-AA)		N-M	kaolin suspension, 1g/L, 100ml	pH 6, 1mg/L with Calcium acetate, 2mM, Transmittance >90%	Rabiee et al. (2014)
	poly (acrylic acid-co-acrylamide) (PAA-c-PACA)		200 kDa and 520 kDa	dissolved organic carbon (DOC)	15 mg/ L PACl with 1 mg/L, turbidity >70%,	Wang et al. (2013)
	PNIPAM-co-AA		N-M	hematite particles	Turbidity remove >90%	Ng et al. (2015)

1.4.3 Non-ionic and amphoteric polyelectrolytes and applications

Non-ionic flocculants interact with colloids via weak force, including hydrogen bonding, hydrophobic attraction and van der Waals force to destabilize particulates. They generated better shear-resistant flocs[43,117–122] and required higher dosage.[121] Two major types of non-ionic flocculants are N-PAM and PEO (polyethyleneoxide). Non-ionic PAM has shown to partially adsorb onto kaolin surface via hydrogen bond.[46] Its conformation falls in between C-PAM: most coiled state and A-PAM: most stretched state, and also enables the flocs to have the largest settling rate.[46]. It was found that polyethylene oxide (PEO) could strongly adsorb with highly acidic oxides

of MO_3, M_2O_5, and MO_2 type, such as MoO_3, V_2O_5, and SiO_2, via the hydrogen bonding between the surface hydroxyls and ether oxygen.[43,118,120,122] PEO displayed a higher affinity and greater adsorbed density than PAM with smectite particles, producing greater particle interactions and stronger networked flocs, which were reflected by higher shear yield stress and better dewatering rate.[43,118] In order to compensate the fragile and costly defect of PEO, a strategy was also made to graft small PEO branched chains onto a high molecular water-soluble PAM polymers backbone which proved to have higher shear stability compared to high molecular weight PEOs.[120]

Different approaches have been utilized to optimize the CF behavior with different types of polymer flocculants. Polyampholyte flocculants, containing both positive and negative charges along the chain have unique interfacial properties including high adsorption to both negatively- and positively-charged particles. The electrostatic charge of amphoteric polymer can be switched from net positive to net negative over a wide pH range, which enables a wider flocculation dosage and pH window. Polyampholytes could either copolymerize through weak acid/weak base monomer, such as methyl acrylic acid and vinyl pyridine, or weak acid/strong base, for instance, methyl acrylic acid and N-subsubstituted allylamines. It has been demonstrated that the flocculants poly-dimethylaminopropyl acrylamide-methacrylamide-acrylic acid (PDMAPAA-MAM-AA), whose electrostatic charge can be reversibly switched from net positive to net negative to provide controlled interactions with the surface of microalgal cells.[99] The synthesis of polyampholytic terpolymers (TP) of methacryloyloxyethyl-N,N-dimethyl-N-benzylammonium chloride (MADAMBQ), acrylamide (AAm), and methacrylic acid (MAS) was performed, and the polymer

displayed greater efficiency in removing anionic dye molecule that was comparable to even the higher molecular weight cationic homopolymer.[123] Pre-formed polyelectrolyte complex (PEC) from two oppositely charged polymers could also "act" as polyampholyte. Complexes with varied combinations have been applied to flocculate fine inorganic particles, with a strong flocculation, large flocs, high velocity of sedimentation, good clarification and no restablization.[124] Details are summarized in the table below.

Table 1.4 Synthetic anionic polymer flocculants, applications and optimal results

Categories	Polymer	Funtional group	Molecular weight	Application	Optimum result	Refs.
Nonionic	N-polyacryadime	Amide	N-M	algal turbid water, NTU:20	pH 4 3mg/L 94.1% Removed pH 9 8mg/L 84.5% Removed pH12 10mg/L 83.7% Removed	Dong et al. (2014)
				phosphorus hematite,NTU, COD	Netural pH, 356mg/L with Ferric Chloride(FC),5.4 mg/L, turbidity almost 100%, COD 90% remove	Yu et al. (2010)
	PEO-g-PAM	Ethylene glycol/Amide	$5.0x10^6$	smectite dispersions, 8%	0.5 mg/g	Besra et al. (2009)
			$5000/5xl0^6$	polystyrene latex	0.5-40 mg/L, 63% remove	Deng et al. (1994)
	PEO	Ethylene glycol	N-M	fines concentration 0.1%	10 mg/g,	Ven et al. (2004)
			$2.5x10^6$	smectite dispersions, 8 wt% solid, turbidity	500mg/kg	Mpofu et al. (2004)
Amphoteric	Poly(maleic acid-co-methylstyrene) (P-MS-c-MeSty) / polydiallyldimethylammonium chloride (PDAMAC) (PEC)	Maletic acid/quatenary amine	$3/3.5x10^4$	clay particle, 2g/L, 97% removal,	0.9 mg/g (n-/n+=0.6), netural pH	Petzold et al. (2009)
	Poly(vinylsulfate)/polydiallyldimethylammonium chloride (PVF/PDAMAC) (PEC)		$2.5/3.5x10^4$		2mg/g (n-/n+=0.2), netural pH	
	polystyrene sulfonate and cationic polyacrylamide (PEC)	Sulfate acid/amide	$1.2x10^6$	alumina particles, 25g/L	50 ppm total polymer, N-M	X.Yu et al. (1993)
	Poly-N,N-dimethylaminopropyl acrylamide-methacrylamide-acrylic acid (PDMAPAA-MAM-AA)	Quaternary amine/acrylic acid	$1.6x10^6$	C. vulgaris cultures at an OD750nm of concentration 5	100% remove for the first time, can be recovered at >98% yields and recycled at least five times	Morrissey et al. (2015)
	N-methacryloyloxyethyl-N,N-dimethyl-N-benzylammonium chloride (MADAMBQ), acrylamide (AAm)and methacrylic acid (MAS)		$2x10^6$	dye blue, 80 mg/L	0.2 mg/L, >90% remove	Guo et al. (2013)

1.4.4 Factors that impact flocculation of synthetic organic flocculants

Crucial factors that influence the flocculation efficiency are molecular weight, charge characteristics and density of the polymer. Details are shown in Scheme 1.1 on the factors that impact the flocculation of synthetic organic flocculants

A higher molecular weight with maximized bridging effect could lead to the formation of larger and stronger flocs.[106] Charge density determines the pathway of polymer adsorption to particle surface. High charged density, polymer adsorbing onto particle surface as a layer has a better charge neutralization capacity but lower bridging ability; lower charge density tends to adopt conformation of loops and tails and link adjacent particle through bridging.[43,46,109,116,118,125] The thickness of the adsorbed flocculants layer was also determined by molecular weight and charge properties.[126] Charged polymers, electrostatic repulsions between chain units prevent the formation of thick adsorbed layers. As a consequence, they tend to adsorb in a flatter conformation with respect to nonionic ones.[115]

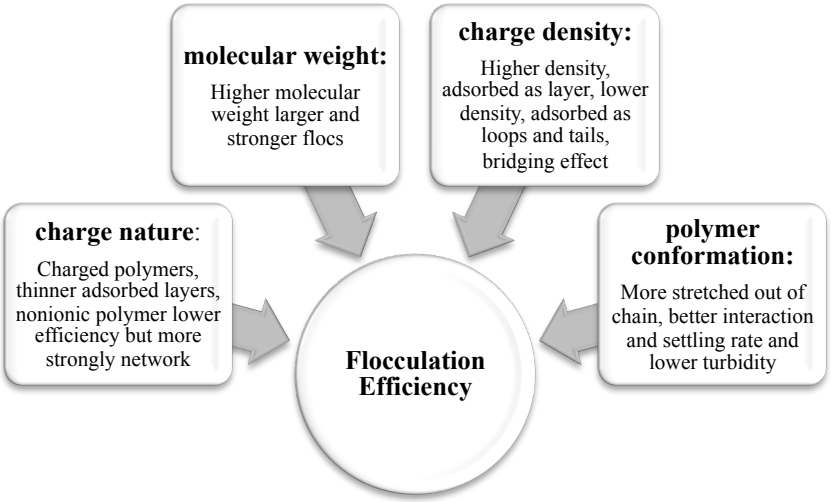

Scheme 1.1 Factors that impact flocculation of synthetic organic flocculants.

For ionic groups, cationic polymer generally shows better flocculation capacity and requires lower coagulants. For instance, cationic polyacrylamide produces more stretching molecular chain in the water that will increase the capacity of adsorption and bridging of suspended particles. A larger yield stress of flocs arising from weak interaction indicated more compact flocs structure and strongly flocs network occurred under weak force interaction[43,118] On the other hand, flocs resulting from electrostatic interaction have a larger and looser structure as well as greater accumulation sludge volume and high membrane fouling.[108] Tailorability also includes polymer conformation such as linear or branched. Three-dimensional model[113] or more extended/stretched out chain structure [118] offered optimum settling rate and lower turbidity.

Briefly, polymer flocculants with effective charge properties, and versatile tailorability advance their universal industrial applications. Compared to inorganic salt, lower dosage and smaller sludge volume generation and well-built flocs network qualify them as a good candidate in wastewater treatment. However, common phenomena can be addressed from polymeric flocculants such as de-stablization/re-flocculation at overdosing range.[125] This seriously impairs the separation efficiency in an operating plant and deteriorates the filtration and dewatering characteristics of the suspension. Toxicity and non-renewability are issues with polymer flocculants.

1.5 Polymer grafted bio-flocculants

The wastewater of industrial effluent treatments requires coagulants/flocculants with high operation efficiency, wide working dosage and pH window, easy handling, inertness to ionic

strength, highly-built flocs network and small amount of sludge residual. However, toxicity and environmental concerns limit the wide use of polymer flocculants. Recently, natural organic flocculants based on natural polymers or polysaccharides, such as chitosan, starch, cellulose, and guar gum emerges as a novel bio-based flocculants. Highlights can be drawn from natural plant-based polymer, as they are biodegradable, nontoxic, widely available from renewable source, environmental-friendly, numerous applications of biopolymer for the wastewater treatment have been discovered and reported.[127,128]

1.5.1 Chitosan

Chitosan is a linear copolymer of D-glucoamine and N-acetyl-D-glucoamine produced by deacetylation of chitin. Chitosan possesses intrinsic positive characteristics from large amounts of primary amine groups along the polysaccharide backbone; long native chain makes it an effective coagulants/flocculants. Chitosan has been successfully applied in pulp mill wastewater,[129] papermaking-processing effluent,[130] dye,[27] mineral,[131][75] chemicals included sewage,[132] removal of organic compounds, inorganic nutrients and bacteria from aquaculture wastewaters[133]. It can also interact with various solid contaminants, ranging from several nanometer length scales to micron size. The unique physico-chemical properties of chitosan render their high affinity with dye molecule, metal ions, humic acid, aromatic derivatives, dissolve organic matter (DOM), total organic carbon (TOC), colloidal particle, suspended solids (SS), bacterial, in different medium.[27,74,134] In addition, an importance part of chitosan has been utilized as a processing flocculants for algae harvesting and thickening.[42,135–138]

Chitosan is a linear hydrophilic copolymer with a rigid structure due to extensive intermolecular and intramolecular hydrogen bonding.[139] Polymer grafting, both from cationic and anionic moieties are effective approaches to increase the hydrophilicity of chitosan and make it water soluble over a wide range.[129] Chen et al. performed a series of polymer modification with chitosan,[57,76,77,140–143] when modification carried on PAM, higher grafting ratio was found to have better performance while also threatened to shield cationic NH^{3+} group on chitosan backbone.[142][141] CMC-g-CTA (carboxylmethyl chitosan-g-3-chloro-2-hydroxypropyl trimethyl ammonium chloride) was tested both in laboratory and pilot scale as an effective flocculant and higher DS (degree of substitute) of CTA yielded a larger working pH range,[77] and the weighting factors determined the overall results such as dosage, mechanical mixing rate and sedimentation time.[143] Research on the flocculation of kaolin and humic acid with CMC-g-PDMC (carboxylmethyl chitosan-g-2-methacryloyloxyethyl) trimethyl ammonium chloride yielded different flocs properties, such as size, fractal dimemsion and floc strength.[76] Carboxylmethyl chitosan (CMC) can also be used the sedimentation of anionic ferric laurate suspension.[144] Phosphorylated chitosan derivatives can be synthesized by P_2O_5 or formaldehyde/H_3PO_3 in water, and the resulting O-phosphorylated chitosan (OPC) and N-methylene phosphonic chitosan (NMPC) have the capacity to reduce the turbidity.[145] NaPAMPS (Poly (sodium 2-acryamido-2-methylpropanesulfonate) copolymerized with TBA (butyl acrylamide) was used as polyanion with chitosan to form PEC (polyelectrolyte complex), which adsorbed on the kaolin surface and protected them from re-dispersion.[146] All the results showed that after modification the

optimum dosage of flocculants were significantly lower than commercial flocculants such as Alum, PAC and PAM as well as the native chitosan.

1.5.2 Cellulose

Cellulose, as the most abundant natural polymer in the world can be a primary chemical resource in the future. Cellulose has a general formula $(C_6H_{10}O_5)_n$, where "n" is from 10 000 to 15 000, is a long-chain of polysaccharide comprised of beta1,-4 linked D-glucose rings, in which every anhydroglucose unit (AGU) is corkscrewed 180^o with respect of its neighbors.[147] Polymer grafted cellulose have been applied for treating dye-contaminated wastewater,[148][149] fine particle clay,[150] sewage treatment,[151][54] heavy metal adsorption and organic pollutants ,[152] ferric laurate suspension.[55]

A variety of cellulose derivatives are produced by chemical modification.[54] Flocculation performance of cellulose xanthate was evaluated by selectively removing metal ions, such as lead and zinc from synthetic wastewater.[150] Specific cleavage of the C_2-C_3 bond of glucopyranoside ring produced two aldehyde groups per unit (dialdehyde cellulose (DAC)).[54,149,151,153,154] This aldehyde group can be further converted to carboxylic acid to form a dicarboxyl cellulose flocculant (DCC) or react with amine group to produce a polycation, both of them were found to be effective flocculants. Girard reagent T ((2-hydrazinyl- 2-oxoethyl)-trimethylazanium chloride, GT) can incorporate quaternary ammonium groups onto the DAC with varied cationicity, the resulting flocculation efficiency approached 85% of the reference polymer (CPAM) with molecular weight $1.5x10^6$ for the removal of ground calcium carbonate (GCC).[154] It is notable that, cellulose

hydrazine, which was obtained from reaction between 2-hydrazino derivatives and DAC, can improve the settling condition of sewage wastewater compared to commercial Zetag (92) polyelectrolyte.[54] Coagulation/flocculation of DCC/$CaCl_2$ exhibited excellent performance in a wide pH range from 4 to 10 with municipal wastewater resulted in a lower residual turbidity and COD in a settled suspension than CPAM.[151] Wu et al. (2014) have successfully introduced 4-vinyl pyridine (4VP) that contained a metal-binding group and butyl methacrylate (BMA), which was used to interact with organic wastes onto cellulose. These two types of polymer on cellulose were demonstrated to have a synergetic effect on heavy metals and organic phenol adsorption.[152] Mishra et al. (2012) grafted a series of polyacrylic acids with different molecular weights onto carboxymethyl cellulose (CMC-g-PAA) for river water clarification, and it was found that higher grafting percent showed maximum flocculation efficiency due to its highest hydrodynamic volume.[155] Bamboo pulp cellulose-graft-ployacrylamide (BPC-g-PAM) on wastewater treatments were investigated by Liu et al. (2014, 2015) and the flocculation behaviors were examined through flocculants treated with kaolin suspension and effluent from paper mill and a surfactant manufacturer, respectively, which can be seen from Figure 1.2.[149,156] Clear phase separation after coagulation/flocculation, and greater removing efficiency qualified the modified cellulose as excellent candidates for the treatment of industrial wastewater.

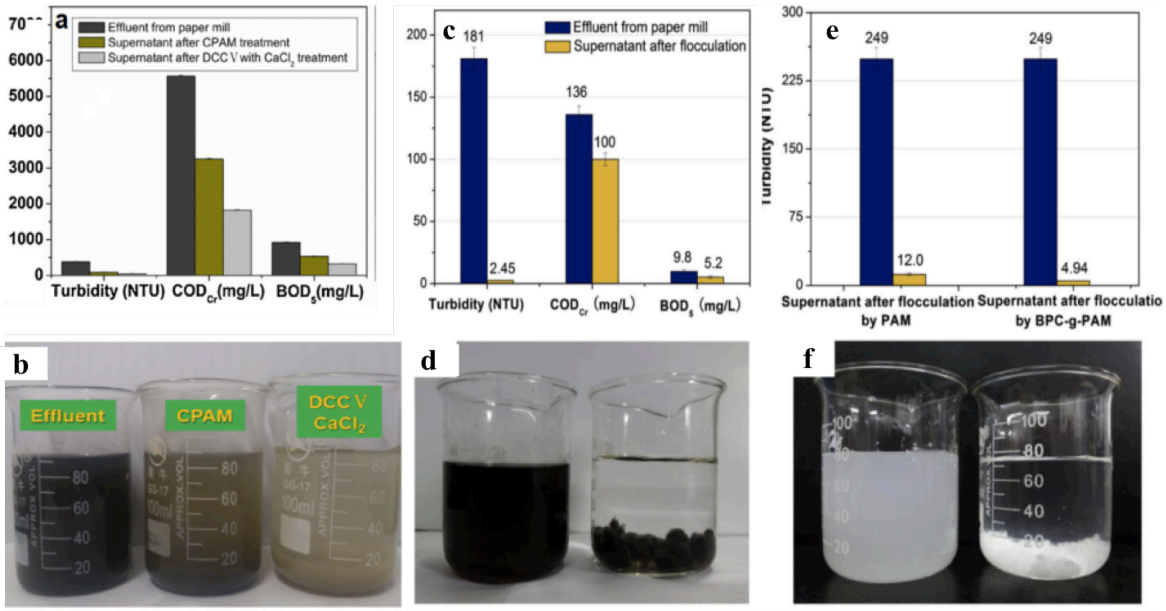

Figure 1.2 Coagulation-flocculation of the commercial CPAM and DCC assisted with $CaCl_2$ with the effluent before and after coagulation-flocculation: (a) turbidity, COD_{Cr} and BOD_5 of the suspensions (c) BPC-g-PAM and PAM treated with the effluent from paper mill (d) BPC-g-PAM and commercial PAM treated with standard kaolin suspension, (b), (d), (f) digital photographs of the suspensions before and after coagulation-flocculation treatment.

More modification approaches can be found in Scheme 1.2, such as epoxy group from cationic quaternary ammonium molecule, and can react with primary hydroxyl group of cellulose, and shown to have notable improvements in flocculation performance with kaolin suspension,[157] ferric laurate[55] and anionic dye removal.[148] Cationic pyridinium groups through 4-(bromomethyl) benzoic acid ([Br][PyBnOO]) and modified cellulose nanocrystals (CNCs) are excellent novel flocculant for Chlorella vulgaris harvesting leading to a significant reduction of water content within the flocs.[72]

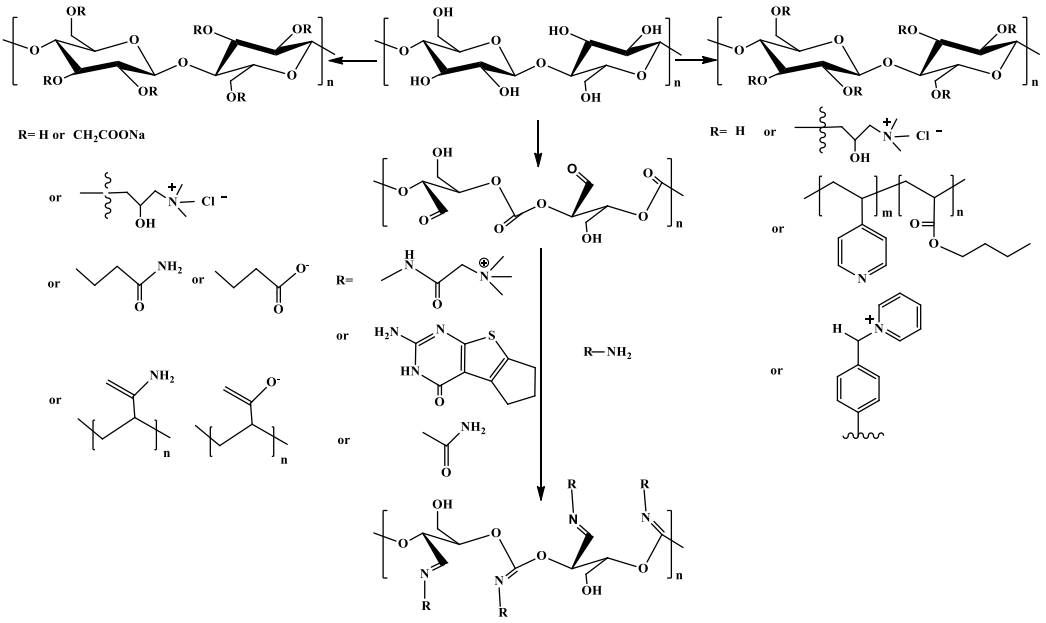

Scheme 1.2 Synthesis of ampholytic/cationic cellulose as bio-flocculants.

1.5.3 Starch

Starch is one of the most abundant and popular natural polymers in the world and has been applied in various fields; an important eco-friendly starch-based flocculants has attracted much attention recently. Starch consists of linear amylose (molecular weight 10,000–60,000) and branched amylopectin (molecular weight 50,000–10^6), which can both be modified as bio-flocculants.[82]

Various ionic moieties have been introduced onto starch backbone through chemical modification. Aly (2002) has prepared and evaluated six types of anionic starch derivatives, as showed in Table 1.5 on ferric laurate particle flocculation. The anionic group, length of the alkyl chain bearing the carboxyl group and chemical formula all have impact on flocculation efficiency.[158] Grafted poly-acrylamide (PAM) and poly N,N-dimethyl acrylamide (PDMA) chains onto the hydroxyethyl starch (HES) backbone displayed a good performance over a wide variety of

metal ion absorption such as, Hg(II), Cu(II), Zn(II), Ni(II) ,Pb(II), whereby all the metals complexed with ligands of HES-g-PAM and HES-g-PDMA exclusively via the carbonyl oxygen atom.[80] Furthermore, a series of starch grafted copolymers, there are PDMC [poly (2-methacryloyloxyethyl) trimethyl ammonium chloride], PDMDAAC [poly(dimethyldiallylammonium chloride)],[159] poly[(acrylic acid)-co-acrylamide],[160] polyacrylic acid,[60] PAM (polyacrylamide),[161] (3- acrylamidopropyl) trimethylammonium chloride (ATMAC),[81] (2-hydroxypropyl)trimethylammonium chloride CTA, [162,163] N-(3-Chloro-2-hydroxypropyl) trimethyl ammonium chloride (CHPTAC),[82] have been demonstrated as effective flocculants in different types of synthetic wastewater in laboratory, such as kaolin and Fe ore suspension, as well as industrial effluents that includes different types of dye, COD, precipitated calcium carbonate (PCC).

In brief, cationic and amphoteric starch flocculants have been developed and their flocculation capability haven been tested mainly with colloidal particles. It is interesting that high water absorbing polymer on starch mainly functioned via oppositely charge interaction between polymer and pollutants when it was applied alone. With the addition of coagulants, it formed polymer complex that can dramatically remove the same charge dye molecule.[159] Cationic modification resulting in lower optimum dosage through quaternizing agent, such as CTA, DMC, ATMAC, DMDAAC, CHPTAC, amine functional group constituted the major cationic moieties. For anionic starch flocculants, inorganic coagulants of $Al_2(SO_4)_3$, $Ca(OH)_2$,or $Fe_2(SO_4)_3$ can change the flocculating agent performance to a large degree, $Ca(OH)_2$ exhibits the most effective coagulant

ability with PAA-PAM-g-starch in term of color removing,[164] the optimum dosage depends on the anionic group according to the trend of carboxyl > phosphate > sulphate by comparing the final transmittance of the supernatant.[158]

Table 1.5 Types of starch-based bio-flocculants applications and optimal results

Starch-based grafted bioflocculants	Treated wastewater	Type of removal	Flocculation efficiency: Optimum dosage (ppm)	Flocculation efficiency: Results	Ref.
carboxymethyl starch	ferric laurate,kaolin suspension	SS, ferric laurate	63	SS remove, final 50%, 54%	Aly (2002)
carboxyethyl starch			60	65%, 74%	
poly(acrylic acid)-starch			43	77%, 83%	
starch-2-hydroxypropylcitrate			40	80%, 87%	
starch-2-hydroxypropylphosphate			35	86%, 90%	
starch-2-hydroxypropylsulfate			7.5	98%, 100%	
poly((acrylic acid)- co-acrylamide)	textile finishing factories effluent	dye, turbidity, initial COD	500 with 1g/ml Ca $(OH)_2$	color reduction 95.4%, COD from 78 to 9	Jiraprasertkul et al.(2005)
starch-g-poly(acrylic acid)				color reduction >90%, COD from 78 to 0	
polyacrylamide-g-hydroxyethyl starch	silica suspension, metal ion	turbidity, metal adsorption	2 for metal, 5 for silica	Hg(II), Pb(II), Zn(II), Cu(II), Ni(II) adsorption percent %: 14, 38, 35, 17, 40	Kolya et al.(2013)
				turbidity: from 275 NTU to 125	
poly N,N-dimethyl acrylamide-g-hydroxyethyl starch				28, 10, 25, 23, 14	
				from 175 NTU to <50	
polyacrylamide-(3- acrylamidopropyl) trimethylammonium chloride-g-amylopectin	kaolin		10	final 5.40 NUT	Kumar et al.(2015)
(2-hydroxypropyl)trimethylammonium chloride-g-carboxymethyl starch	kaolin, hematite suspension	turbidity	0.25 at pH 4 0.60 at pH 7 0.80 at pH 10	residual Transimittance 92.8% residual Transimittance 97.2% residual Transimittance 97.7%	Li et al.(2014)
N-(3-chloro-2-hydroxypropyl) trimethyl ammonium chloride-g-carboxymethyl starch	kaolin suspension		1 at pH 4 1 at pH 7 0.80 at pH 10	residual Transimittance > 90%	Pal et a.l (2004)
N-(3-chloro-2-hydroxypropyl) trimethyl ammonium chloride-g-starch	silica suspension		0.5	final turbiddity 4NTU	Sagar et al.(2012)
amylopectin-graft-polyacrylamide-graft-polyacrylic acid	Fe ore suspension		2.5	from 126.7 to 4 NTU	Pal et al.(2012)
starch-graft-poly(methacryloyloxyethyl) trimethyl ammonium chloride	kaolin suspensions		1	near 0 NTU	Wang et al.(2013)

1.6 Summary and discussion

Various types of wastewater has been utilized in different wastewater applications including

oil-contaminated refinery sludge, domestic waste disposal, polymer manufacturing plant effluent, tannery wastewater, pulp mill discharge, municipal sewage, acidic coal mine drainage as well as textile industry waste. The corresponding flocculation behaviors of coagulants and flocculants of metal salt coagulants, polymeric inorganic and organic hybrid coagulants, synthetic organic polymer and polymer-grafted bio-flocculants have been investigated in terms of removing TS, BOD, COD, TOD, NOM, dye molecular, chemical organic pollutants, hazard metal ion, suspended colloidal and microalgae harvesting. The advantages and defects are summarized in Table 1.6 below.

Table 1.6 Summary of advantages and defects of various coagulants/flocculants

Type	Advantages	Defects
Inorganic metal salts	Cost and energy effective, easy to operate	Uncontrolled hydrolysis, fast precipitation and lower efficiency, high sludge volume, loose floc fracture, poor dehydration
Polymeric inorganic and organic hybrid coagulants	Lower residual metal-ion, favorable colloidal charge neutralization, considerable bridging effect	Affected by inorganic species distribution, physical parameters, charge density, sensitive to pH
Sythetic organic polymer	Versatile tailorability including molecular weight, ionic charge nature and density; flexible polymer structure; low dosage	Narrow operation usage and pH window, restabilzition at overdosing, toxicity, non-renewable
Polymer grafted bioflocculants	Renewable source, environmental-friendly, lower polymer amount required, high natural polymer weight, wider pH and dosage working window, inert to environment	High dosage, increase activated sludge volume, limited tailorability

By controlling the pH, pre-hydrolyzed inorganics can selectively generate desire polymeric species with higher molecular weights and cationic charges, while the working efficiency could fluctuate easily with different wastewater sources. Incorporating silicates into inorganic coagulants enhance the colloidal stability of coagulants/flocculants by sacrificing the net cationic charges. Molecular weight and intrinsic viscosity of inorganic/organic hybrid polymers are key factors that

affect the flocculation performance when grafting polymer onto inorganic coagulants. Higher molecular weight always implies higher operation cost; and this is also a crucial factor in synthetic organic polymeric flocculants. Markedly, the cost differential between organic and inorganic coagulants can be enormous, with average costing five times more. Nonetheless, many choose the more costly polymers, because they are advantageous in several aspects, such as lower usage, better separating rate, a wider waters range, lower sludge volume. On the other hand, the water-quality issue is inevitable concerning toxicity of cationic polymer and potential environmental risk to human health. The demand for environmental friendly technologies in industry using functionalized natural material advances the development of sustainable materials. Biopolymer based flocculants preserve the natural high molecular weight and versatile functionality. By grafting the polymer onto natural polymer surface, it improves the flocculants characteristics. The molecular weight of grafting polymer plays a minor role compared to the molecular weight of biopolymer itself. Biopolymer also satisfies several critical requirements for commercialization, such as sustainable resource, stable and easy handling properties. Other advantages of bio-flocculants include their high removal efficiencies, considerable denser flocs due to the polysaccharide backbone to populate the net-like flocs structure and wider pH and working dosage window. Meanwhile, deficiencies also exist in these novel flocculants, due to their polysaccharide chains, its biodegradable risk may also result in large volume of activated sludge. The economic cost of processing and lower optimum dosage amounts should be taken into account in order to populate bio-flocculants in common wastewater treatments.

Although most of the flocculants have been proven to be effective in the wastewater in laboratory scale, there is still a great need for trials in operating pilot plant of a wider variation of pH, ionic strength, and different types and concentration of contaminants in wastewater with regards to their performance in industry. The working efficiency of inorganic metal salt coagulants depends greatly on pH of the solution which dominants the species of metal cations, and fundamental studies of coagulation chemistry is required to determine the operation conditions. Furthermore, the discharged water needs to satisfy the environmental legislation both for residual alumina and pollutant concentration.

Chapter 2. Cationic Cellulose Nanocrystals (CNCs) for Organic Colloidal Latex Particle Flocculation

2.1 Introduction

The aim of coagulation-flocculation (CF) treatment is primarily to remove the colloidal matter, which is present in wastewater. Recently, CF technology also exhibits great potential the applications of heavy metal adsorption,[14–17] microalgae harvesting,[18–21] removal of dye [22–28] and organic matter.[29–36] Flocculants play an important role in the industrial solid-liquid separation, municipal sewage treatment, mineral processing effluent and petroleum refinery.[165]

Colloidal particles are well-known for high adsorption, long-term stability and high dispersibility, by virtue of their nanometer-sized and large specific surface area.[37] Their charged surfaces enable them to repel each other and allow for their high mobility in solution. The basic principle of coagulation is to aggregate small particles into large compounds so that the impurities can be removed by subsequent solid-liquid separation.[13] Upon the addition of flocculants, the destabilized small aggregate can be brought into macrofloc, where the hydrodynamic shear force can no longer overcome the gravity. As a result, the macrofloc will precipitate from the solution and solid-liquid separation will occur. [38]

Various coagulants and flocculants can be categorized into inorganic metals salts, organic synthetic polymers, and polymer-grafted bio-flocculants. The common problem caused by inorganic coagulants is that the flocs are generally voluminous, fragile and have low resistance to

shear, which increases the difficulty of subsequent settling and phase separation.[166] Polymeric flocculants are more effective and versatile in producing large shear-stable flocs. However, these flocculants are primarily petroleum-based and non-renewable; thus, the toxicity with cationic polymers limits their universal application in wastewater treatment. Additionally, many factors such as molecular weight, chain length, charge density, conformation, functional group of polyelectrolytes could render flocculants impotent.[102]

Recently, the growing concern of environmental effects and health risks due to inorganic/organic coagulants have generated interests in the development of more sustainable alternatives, such as polyelectrolyte-grafted, natural polymers that include cellulose,[70–72] chitin,[73,74]chitosan,[75–78] starch[79–82] and their derivatives. Grafting has greatly reduced the amount of polymer required to achieve flocculation efficiencies comparable to previously developed flocculants.

Cellulose, the most abundant natural polymer in the world, can be a primary material resource in the future. Cellulose has a general formula $(C_6H_{10}O_5)_n$, where 'n' is between 10,000 and 15,000; a long-chain polysaccharide comprised of beta-1, 4-linked D-glucose rings.[147] Acidic hydrolysis can cleave the amorphous region and the residual will form cellulose nanocrystals (CNCs); a rod-shape possessing dimensions of 5-20 nm width by 200-400 nm length. CNCs are facile to fabricate, biocompatible, biodegradable, yet thermally and chemically stable.[167] Polymer grafted celluloses have been widely used in dye contaminated waster,[148] fine particle clay,[150] sewage treatment,[151] heavy metal adsorption and organic pollutants.[152] Surface modification such as, epoxy containing quaternary ammonium polymers can attach with primary hydroxyl group on cellulose surface

through hydrolysis. Free radical polymerization can also graft polymer from cellulose surface, such as polyacrylamide (PAM), polyacrylic acid (PAA). Recently, our group has demonstrated that modified cellulose nanofibrils with quaternized ammonium group is an effective flocculant for azo-dye removal.[148]

However, developing CNCs as novel flocculants remains an underexplored area. An application of CNCs can be found in grafting cationic pyridinium groups onto cellulose nanocrystals (CNCs) as a novel flocculant for harvesting Chlorella vulgaris. This study significantly reduced the second dewatering step by lowering the water content in flocs.[44] It is reasonable to forecast that developing the nano-structure via surface modifications and increasing the aspect ratio will promote bio-flocculants in the near future. We endeavor to explore the untapped potential of CNCs as novel flocculants. Three different types of amine-containing monomers i.e. N-N-(dimethyl amino) ethyl methacrylate (DMA), 4-vinylpyridine (4VP), polyamine, were grafted from the CNC surface. Acrylate latex particle was used as a model organic colloid. The effects of different kinds of amine groups, pH and mixing ratio of amine groups on CNCs to carboxylic acid groups on latex particle were examined. Flocculation mechanisms are discussed in details.

2.2 Experiment

2.2.1 Materials and Instrumentation

Cellulose nanocrystals hydrolyzed from wood pulp with an average charge density of 0.26 mmol/g was provided by Celluforce Inc. N-N-(Dimethylamino) ethyl methacrylate (DMA), epichlorohydrin (EPH), dimethylsulfoxide (DMSO), tetrabutylammonium hydroxide (TBAH),

ammonium hydroxide (28-30% NH_3 in water), 4-vinylpyridine (4VP), cerium (IV) ammonium nitrate (CAN) and ammonium persulfate (APS) were purchased from Sigma Aldrich.

Hydrochloric acid (HCl 1.0 M) solution and sodium hydroxide (NaOH 1.0 M) solution were prepared from standard solutions by dilution. Water (≥ 18 MΩ cm) used in all procedures was filtered through a Millipore Mill-A purification System.

2.2.2 Sample synthesis

Suspension of PDMA-g-CNCs was prepared as previously described.[168] CNC (2.0 g) was dissolved in 200.0 mL water in a 500 mL three-necked flask, and the resulting solution was purged with N_2 for 1 h. DMA (2.0g) that was passed through an alumina oxide column to remove the inhibitor that was slowly introduced into a reaction flask, and followed by the addition of the initiator (APS, 300.0 mg). The reaction mixture was subsequently heated at 70 ^oC for 3 h.

Suspension of P4VP-g-CNCs was prepared as described in the literature.[56] 4VP was passed through an alumina oxide column to remove the inhibitor. CNC (1.0 g) was dissolved in 100.0 mL water. 1.875 mL 70wt% HNO_3 and 2.85g 4VP monomer were added to the CNC dispersion. Under N_2 atmosphere, the reaction mixture was sonicated continually for 1 h in an ice bath. Then 0.375 g CAN dissolved in 1.0 mL degassed water was added to activate the reaction. The reaction mixture was sonicated for another 2 h, followed by stirring overnight.

Amine functionalized CNCs was prepared as follows: 2.0 mL epichlorohydrin was dropwise added into a flask containing ammonium hydroxide (5.20 ml) and then the solution was refluxed at 65 ^oC for 2 h. A reflux condenser was used in order to keep ammonium vapors from accumulating.

Simultaneously in another flask, CNCs (1.37 g) were dispersed in DMSO (90.0 mL), and TBAH (2.19 g) was added into the solution with the molar ratio of TBAH/AGU of 1.0. The epichlorohydrin solution was dropwise added into the CNC solution, while the temperature was maintained at 45 ^{o}C with constant stirring for 3 h.

After the reaction, the modified CNCs were purified as follows: the reacted mixture was concentrated via centrifugation at 9000 rpm for 15 minutes, then rinsed with water; this was repeated three times. The solution was re-dispersion in water, then dialyzed (M_W cutoff of 12,000 Da) against deionized water for at least one week until the water conductivity of the dialysis remained constant. The purified solution was subsequently concentrated and lyophilized for further application.

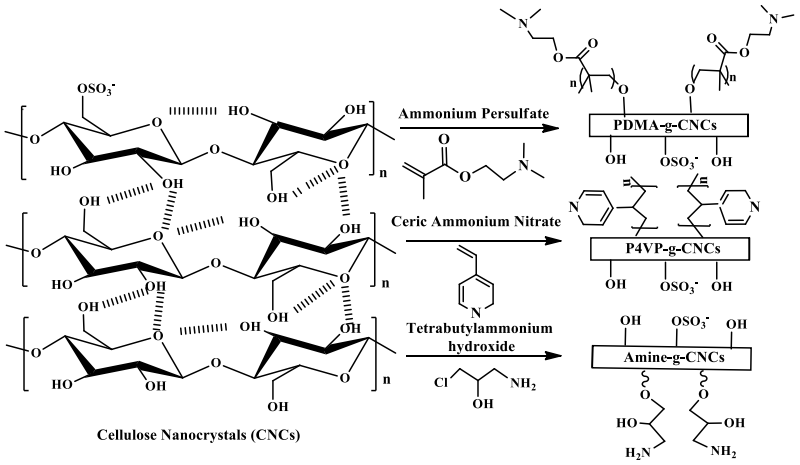

Scheme 2. 1 Synthesis of PDMA-*g*-CNCs, P4VP-*g*-CNCs and amine-CNCs.

2.2.3 Characterization

Fourier-Transform Infrared (FT-IR) Spectroscopy

FT-IR spectra of PDMAEMA-*g*-CNCs, amine-CNCs, P4VP-*g*-CNCS and pristine were recorded on the Bruker Tensor 27 spectrometer FT-IR spectrometer at a resolution of 4cm^{-1}. 64 scans between 400 cm^{-1} to 4000 cm^{-1} were collected for each sample. Test pellets were prepared by grinding and compressing approximately 1% (w/w) of the sample in KBr.

Zeta-potential (ZP)

The ξ-potential of cationic CNCs samples were measured using a Malvern Nano-ZS90 Zeta sizer at room temperature. The concentration of the samples was 0.1% by weight. Three repeated measurements were conducted for each sample.

Potentiometric and conductometric titration

The amine groups within both the functionalized CNCs and the latex particle were quantified by conductometric titration using a Metrohm 809 Titrando autotitration. Typically, 50.0 mL of functionalized CNCs water solution was gently stir at 25 ^{o}C. 0.02 M NaOH was used as standard titrant dosing into sample vial at a rate of 0.05 $mLmin^{-1}$. The conductivity and pH as function of titrate volume was recorded.

2.2.4 Flocculation experiments

The latex was prepared in our lab via emulsion polymerization, with hydrodynamic radius around 100 nm. Stock solution of latex (1.0 g/L) and flocculants were freshly prepared before each flocculation test, which was conducted in a 7 mL glass vial at room temperature. Modified CNCs flocculants were rapidly mixed with latex suspension at 200 rpm for 2 minutes for the formation of floc, followed by slow mixing at 50 rpm for 5 minutes, settling overnight before collecting

supernatant for transmittance analysis, floc for ZP and size measurements respectively. The flocculation efficiency is expressed as Equation (2.1).

$$\text{Flocculation Efficiency} = 1 - \frac{w_{\text{supernant}}}{w_{\text{blank sample}}} \times 100\% \qquad (2.1)$$

$W_{supernant}$ and $W_{blank\ sample}$ are the solid content in the latex suspension with and without flocculants treatment, respectively. This can be calculated through optical density of suspension, which is proportional to the solid content of suspended colloids in the solution. The calibration curve under pH 4, 7, 10 were performed by monitoring the sample transmittance at wavelength 500 nm in a UV-visible spectrophotometer over a wide range of latex concentration. Then, the supernatant transmittance of latex suspension were measured after flocculation in all the three pHs were measured, the values were converted into solid content based on calibration curve. The flocculation efficiency is the percentage of colloids that has been settled down to the bottom. Flocculation window is defined as the flocculation efficiency near 100%, and the optimal dosage is the lowest mixing ratio value.

Floc size and zeta-potential measurements

Floc surface charge and size were analyzed by dynamic light scattering using a Malvern Nano-ZS90 Zeta sizer. After mixing of each sample, the floc was charged and diluted five times using water to prepare a suspension. Then it was tested for surface charge properties and size through its respective protocol. The floc size is defined by volume-weighted mean diameter (D_v), both of the value were calculated and provided by the data processing software.

2.3 Results and Discussion

2.3.1 Characterizations of polymer grafted CNCs

Polymer grafted CNCs were characterized using FT-IR and the spectra are illustrated in Figure 2.1. For PDMA-*g*-CNCs, the peak at 1640 cm^{-1} due to the vibration of CNCs, which has disappeared and a new characteristic peak 1728 cm^{-1} corresponding to the stretching of C=O bond on PDMA chains was observed, indicating that the PDMA was successfully grafted onto CNCs. In the case of P4VP-g-CNCs, the small peaks at 1606 cm^{-1} and 1377 cm^{-1} are assigned to the stretching of C=N bonds of the pyridine or pyridinium ion group. This result indicated the polymer was successfully grafted on the CNCs surface. In the spectrum on amine-g-CNCs, the peak at 1640 cm^{-1} disappeared which suggested the hydroxyl groups were successfully substituted, and the new peaks displayed at 1571 cm^{-1} and at 1345 cm^{-1} are attributed to the N-H bending and C-N bending of amide I, respectively. In addition, the peak at 3500 cm^{-1}, corresponding to the N-H stretching of primary amine overlap with O-H stretching in CNCs.

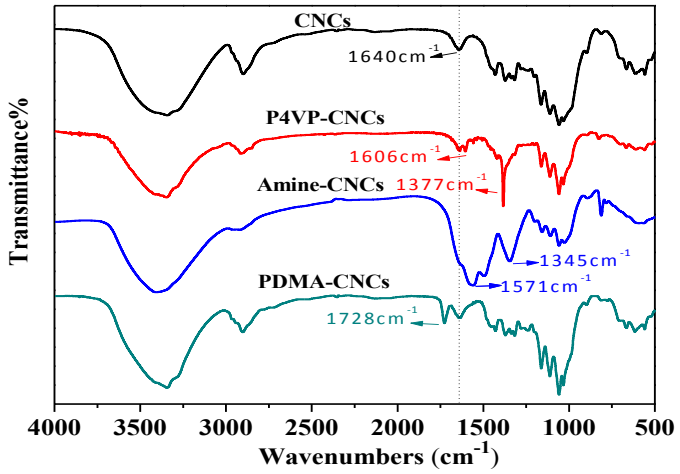

Figure 2.1 FT-IR spectra of CNCs, PDMA-g-CNCs, P4VP-g-CNCs and amine-g-CNCs.

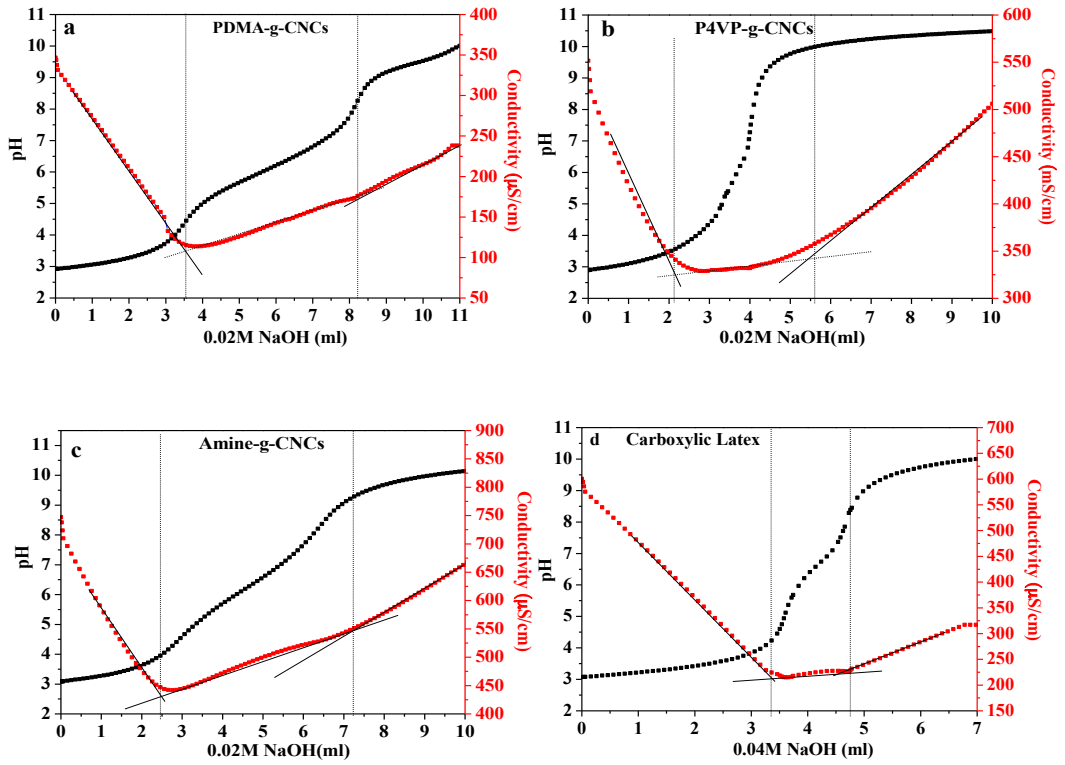

Figure 2.2 Conductometric titrations of (a) PDMA-g-CNCs, (b) P4VP-g-CNCs, (c) amine-g-CNCs and (d) carboxylic acid latex with sodium hydroxide.

The amounts of amine groups present in the functionalized CNCs were quantified by conductometric titration using the NaOH standard titrant. The addition of NaOH into modified CNCs solution will first neutralize free proton ion, resulting in an increase of pH and a decrease in the conductivity (First stage). When the pH of the solution approached the pKa of amine functional group, the OH^- started to react with conjugate acid on the CNCs surface. As a result, conductivity curve entered into the plateau region until all the functional group on CNCs were completely

deprotonated (Second stage). Continual dosing of NaOH titrant will induce a fast increase of the conductivity resulting from the dissociation of titrant (Third stage). The region between the two vertical lines displayed in Figure 2.2 corresponds to the amounts of the amine groups. The three modified CNC samples and carboxylic acid amount on latex particle were analyzed using the same protocol.

Zeta potential results are summarized in Figure 2.3. Pyridine, PDMA and polyamine are polyelectrolytes with the pKa of 5.2, 7.4 and 9.3 respectively; the basicity of amines is increased with the increasing of its pKa value. A higher pKa value corresponded with a stronger conjugate base and the strength of base follows the order of pyridine < tertiary amine < primary amine.

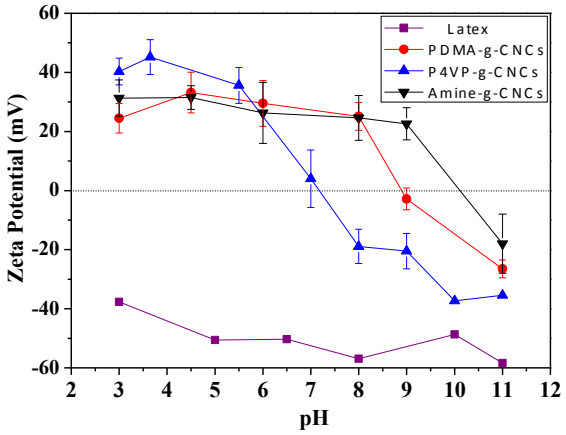

Figure 2.3 Zeta potential value of PDMA-g-CNCs, P4VP-g-CNCs, amine-g-CNCs and carboxylic acid latex samples.

This can be observed from Figure 2.3, where all the three modified CNCs flocculants exhibited a positive to negative transition when pH were close to their pKa. At the pKa of amine group, the ionic group was protonated and yielded a positive ZP value, when pH became higher than its pKa,

deportation of amine function group will occur and CNCs residual sulfate ester group was then manifested and provided a negative ZP signal. The carboxylic acid group gave an intensified negative trend over the whole pH range.

The amounts of different groups present in the CNCs based material can be quantified by conductometric titration using NaOH standard titrant. The titration results of carboxylic acid latex, PDMA-g-CNCs, P4VP-g-CNCs, amine-g-CNCs are summarized in Figure 2.4.

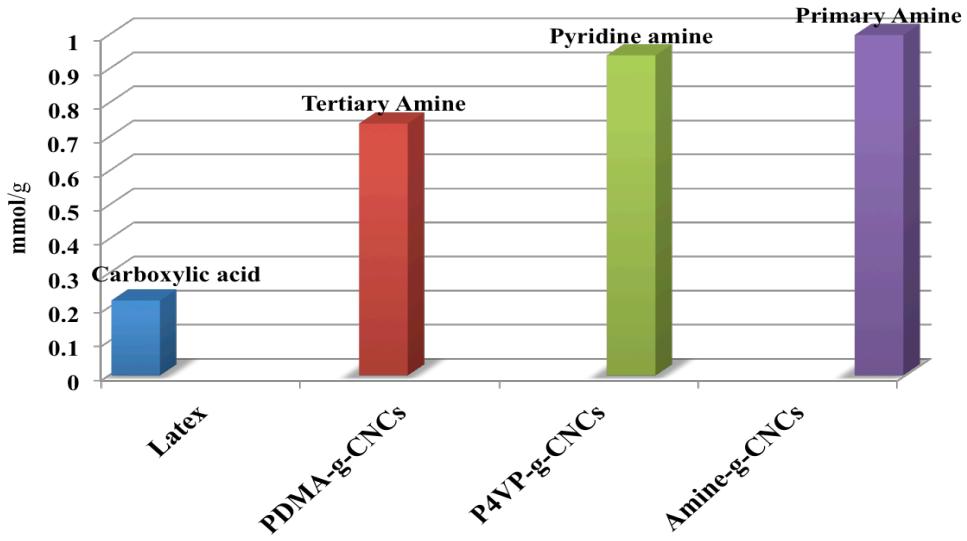

Figure 2.4 Summary of different types and amounts of functional group both in cationic CNCs and anionic latex.

2.3.2 Flocculation performance

Since the flocculants dosage and pH are the two main parameters that will affect the flocculation efficiency, the flocculation performances of cationic CNCs were therefore systematically evaluated at various dosages under acidic (pH=4), neural (pH=7) and alkaline (pH=10) conditions. In order to

quantify the flocculation efficiency, the relationship between a series solid content of latex suspension and their corresponding transmittances were established from the calibration curve shown in the Figure 2.1.

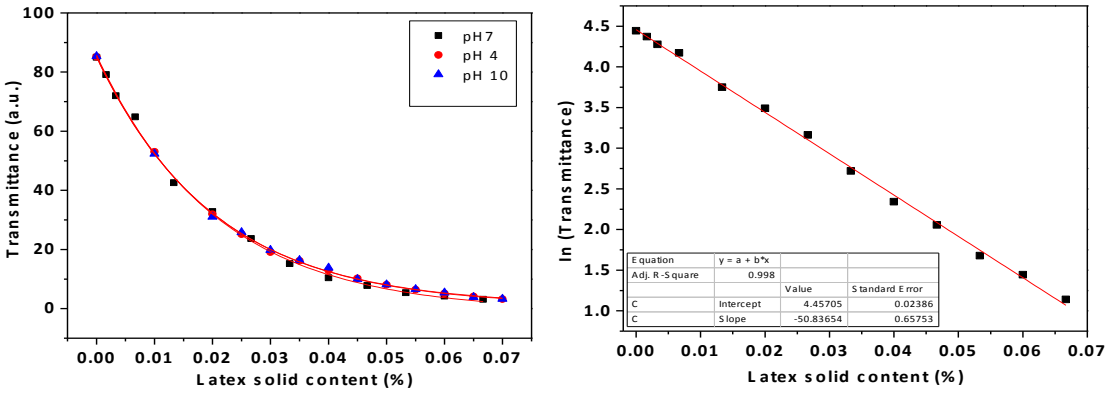

Figure 2.5 Calibration curve of solid content with transmittance under pH 4, 7 and 10.

The calibration curve of three pHs overlapped with each other, which indicated that the pH did not affect the relationship of transmittance and solid content. The sample's supernatant transmittance was substituted into the universal calibration function to calculate the residual solid content. Flocculation efficiency is defined as the solid content that is removed through the flocculation process, which was calculated according to Equation (2.1). The flocculation window describes a range of dosage where all the latex colloids have settled down and the optimum dosage occurred at the lowest flocculants dosage.

2.3.2.1 Effects of pH

The pH effect on the flocculation efficiency (FE) was studied by measuring the transmittance of the supernatant after flocculation. Figure 2.6 provides a visual picture after latex was mixed with

the flocculant PDMA-g-CNCs and allowed to settle overnight. By measuring the transmittance of each supernatant, the flocculation efficiency was calculated in Figure 2.6b, which is consistent with observation from Figure 2.6a.

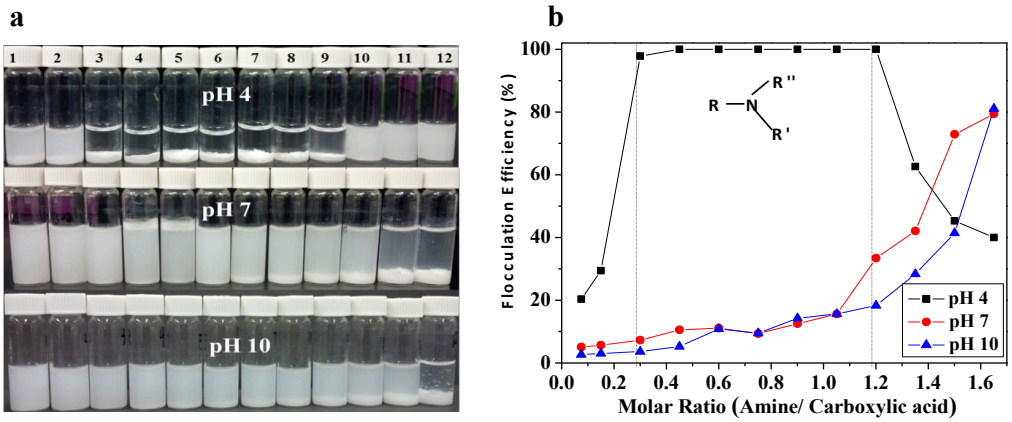

Figure 2.6 Flocculation efficiency of PDMA-g-CNCs with latex suspension with various mixing ratio under three different pHs (a) Digital pictures of sample after flocculation and 24h; (b) flocculation efficiency results calculated from UV-vis transmittance.

At pH=4, a wide flocculation window was obtained when the mixing ratio of amine and carboxylic acid fell into the range of 0.26 to 1.05, where all the latex particles have been settled down to the bottom and a clear supernatant was observed. In acidic condition, the PDMA-g-CNCs flocculants were protonated to acquire a positive charge, and the steric repulsion of the intermolecular chain will extend the polymer chains into solution. This enabled a strong interaction and increased collision frequency between positively charged flocculants and negatively charged latex particle. On the other hand, the latex particles were partially deprotonated at pH 4, which may explain why only at a molar ratio 0.2 (which was far from stoichiometric ratio of functional group),

the latex was completely settled down to the bottom. However, excess cationic CNCs absorbed on the latex colloid and induced a re-stabilization due to the reversed charge repulsion.[131,169]

At pH of 7, the flocculation window disappeared and the optimal mixing ratio shifted to a larger value. Partially protonated PDMA-g-CNCs reduced the net positive charge density, and polymer tended to coil on CNC surface.[170] In the same manner, increasing pH will also improve the negative charge density via carboxylic group deprotonating which enlarged the electrical double layer of latex colloid.[171] This synergistic effect caused a decrease of overall flocculation efficiency, therefore even under the maximum mixing ratio, only 80% flocculation was achieved.

When the pH was increased to 10, all amine functional groups were deprotonated, and the polymer chains collapsed onto CNC backbone and the surface charge became negative. Induced the swelling of the latex shell with sufficient countering ion occupying the electrical double layer.[172] The flocculation phenomena can be observed either from the sediments at the bottom of the vial of the figure. A possible reason could be related to the hydrogen bond from carbonyl group of PDMA acting as a driven force for the adsorption on the latex particle.[173] van der Waals interaction between hydrophobic CNC surface with latex particle promoted the latex agglomeration to form macroflocs. Micrographs of P4VP-g-CNCs samples after mixing and settling with latex colloids and the flocculation efficiency results are shown in Figure 2.7.

At pH 4, P4VP modified flocculants possessed narrower flocculation window ranging from 0.15 to 0.30, with an optimal mixing ratio of 0.15. The flocculation efficiency decreased to 60% and fluctuated around this value. The polymer underwent a similar conformational change with respect

to PDMA on CNCs. Pyridine group protonated as pyridinium ion, which is a weaker base than tertiary amine,[174] resulting in a narrower flocculation window.

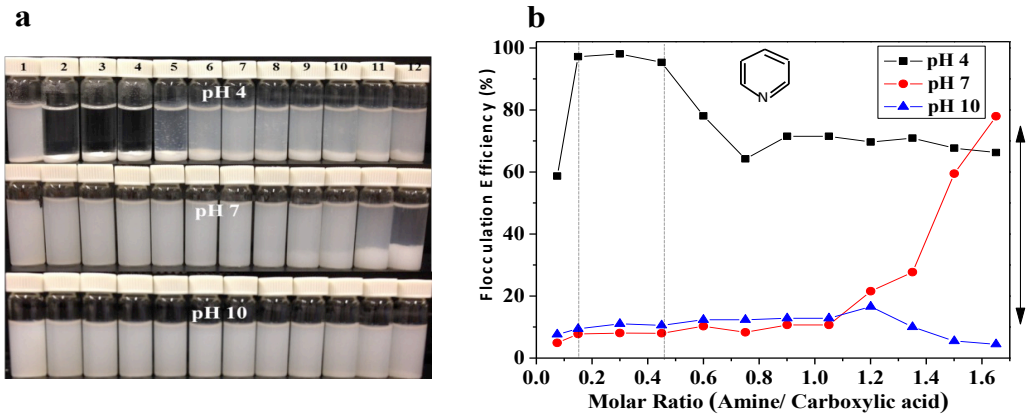

Figure 2.7 Flocculation efficiency of P4VP-g-CNCs with latex suspension with various mixing ratio under three different pHs (a) Digital pictures of sample after flocculation and 24h; (b) flocculation efficiency results calculated from UV-vis transmittance.

By increasing the pH to 7, which is above its pKa, the pyridine will be completely protonated, and the polymer secondary structure was interrupted, flocculation phenomenon can still be observed at high mixing ratio. The van der Waals attraction between the π-conjugate of pyridine groups and latex particles were ascribed as the driven force to particle bridging,[175] and the hydrophobic CNC surface will promote latex particle aggregation. However, by increasing the pH to 10, the surface charge of P4VP-g-CNCs became negative, and the residual sulfate ester groups from CNCs impart a negative repulsion between the flocculants and latex particle, no flocculation was observed at pH 10.

In the case of amine-CNCs, at pH 4, the optimal mixing ratio was continually shifted to a lower value and the flocculation window was further diminished. It is reasonable that, the strongest

interaction from primary amine gave a lowest optimal dosage. However, the latex suspension became turbid again when mixing ratio was increased to 0.3, demonstrated the stronger interaction from primary amine group can also impaired the flocculation efficiency and narrowed flocculation window.

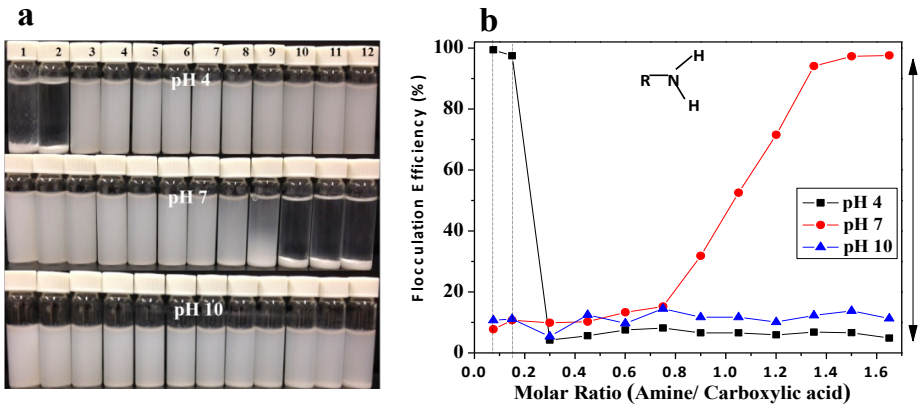

Figure 2.8 Flocculation efficiency of Amine-g-CNCs with latex suspension with various mixing ratio under three different pHs (a) Digital pictures of sample after flocculation and 24h; (b) Flocculation efficiency results calculated from UV-vis transmittance.

When the pH was increased to 7 which is under pKa of primary amine, the major functional groups were preserved as the protonated state slightly reduced the charge density,[176] and flocculation window emerged again from 1.2 to 1.66. It is noticeable that, the strongest base of primary amine group yielded the best performance under neutral pH due to the greater interaction between primary amine groups and carboxylic acids on the latex. No flocculation was detected at pH 10, which implied the flocculation capability is very much related to the state of the primary amine group and the conformation of the polymer chains.

2.3.2.2 Floc properties

Primarily, two parameters of floc, ZP and Zeta size, were investigated and compared under a series of mixing ratio in order to elucidate the flocculation process and possible mechanism. The results of PDMA-g-CNCs are summarized in Figure 2.9.

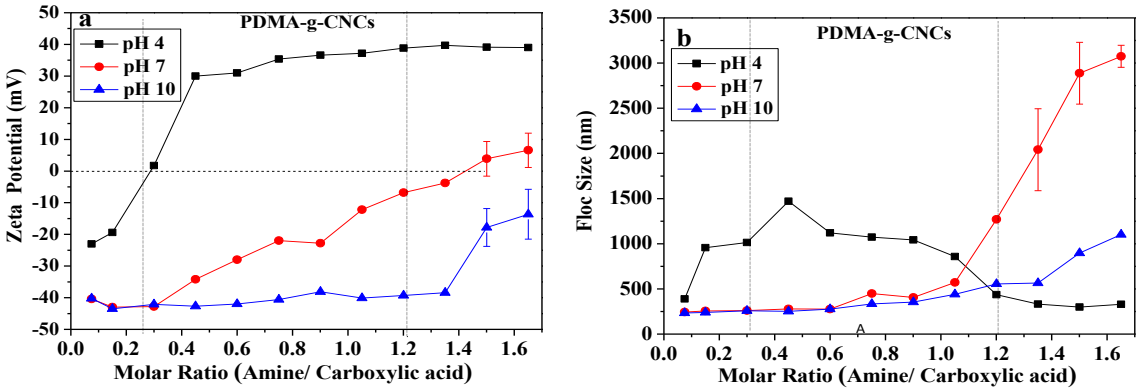

Figure 2.9 Floc properties under three different pHs from PDMA-g-CNCs flocculants (a) Zeta potential value and (b) Floc size.

It is interesting to notice that at pH 4, ZP approached zero at the optimal mixing ratio, where it then reversed to be positive. This suggested that charge neutralization played a dominant role in destabilizing the colloidal particles.[42,101] Due to the extensive polymer structure and high charge density, PDMA polymer was able to rapidly coat onto the negatively charged latex particle surface, and agglomeration mainly occurred via the shielding of steric repulsion that induced the particles to form microfloc. Floc surface charges were sustained with an increasing positive trend, and the floc size fluctuated around 1000 nm within the flocculation window. When the mixing ratio was raised beyond 1, the reversed charge repulsion became strong enough to prevent the destabilized particles from coming together and manifested a decrease of floc size in Figure 2.9b. The optimum dosage at

pH 7 occurred at the maximum amount, where the floc was found to be neutral and floc size reached the maximum. It was believed that the partially deprotonated polymer can adsorb onto latex particle surface either in the "loop and tail" or in the "patch" pattern, depending on the charge density and molecular weight.[119,177] In order for bridging effect to occur, the "dangling" polymer chains consisting of loop and tail need to be long enough to "bridge" the colloidal particles.[106] For the polymer grafted CNC flocculants system, it was possible that "particle bridging" occurred by taking advantage of CNCs crystalline backbone and promoting particle agglomeration. It is obvious that the flocs at pH 7 have a much larger size compared to flocs at pH 4, which is consistent with the proposed flocculation mechanism on the bridging effect that produced a larger size than charge neutralization pathway.[106] Hydrogen bond form with the carbonyl groups of PDMA can also facilitate floc aggregation at pH 10 when all the ionic functional groups were protonated,[121] and the floc size can still increase to 1000nm with slightly negative surface charge.

The results of P4VP-g-CNCs are summarized in Figure 2.10. At pH=4, the floc surface exhibited negative charge with similar floc size of 1000 nm at the optimum dosage, charge neutralization mechanism was less obvious in the weaker base of pyridine amine under acidic condition. This suggested that destabilized particle originated through the oppositely charge attraction, due to the steric hindrance of heterocyclic ring of pyridinium ion that prevented effective contacts between pyridinium ions and carboxylic acid groups on the latex.[123] The larger floc size distribution at pH=4 also indicated the insertion of hydrophobic ring into flocculants that may contribute to the larger floc structure.[123,178] The residual turbidity at pH 4 in high dosage region were assumed to be

the loose and large floc structure which contributed to the partially settlements. Increasing the pH to 7 (near the pKa of pyridine group), the protonated ionic group lost its functionality and diminished the flocculation capability. No flocculation was observed at pH 10, and the flocs sizes were kept at the same level.

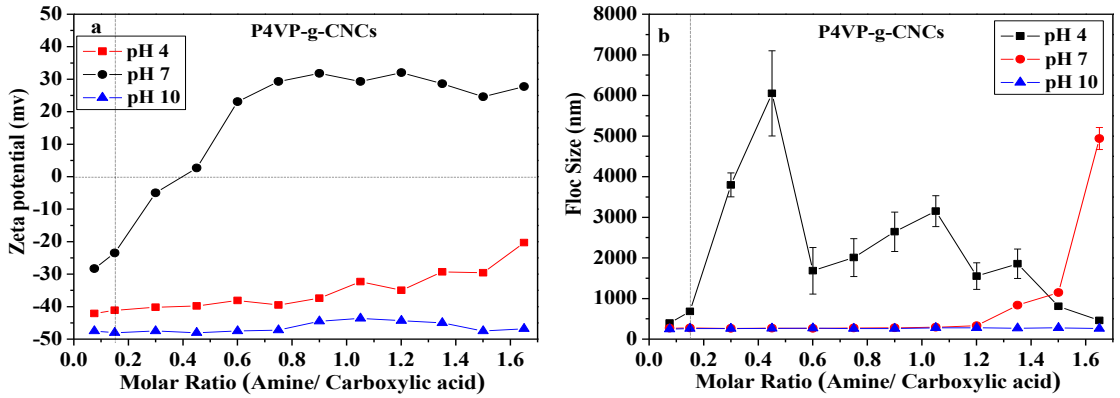

Figure 2.10 Floc properties under three different pHs from P4VP-g-CNCs flocculants (a) Zeta potential value (b) floc size.

The results of amine-g-CNCs are summarized in Figure 2.11. As was observed earlier, the latex particle was fully settled at the lowest mixing ratio, which displayed a zero net charge at pH=4. This also coincided with the "charge neutralization", where an instant charge reverse occurred after the optimum dosage that a re-stabilize the flocs. At pH=7, it was found at the optimal molar ratio of around 1, the flocculation produced neutral floc, and the flocculation window reappeared. The surface charge was shown to have a negative to positive transition and the floc size spontaneously increased. For the primary amine groups, the majority of surface functional group and polymer structure are preserved. The high amount of amine groups could interact with carboxylic acid groups on the latex, and the extended polymer structure may also facilitate "bridging" that connect

the particle to CNC surface. When the ionc group lost its functionality, no flocculation occurred at pH=10, as indicated by the floc charge and floc size.

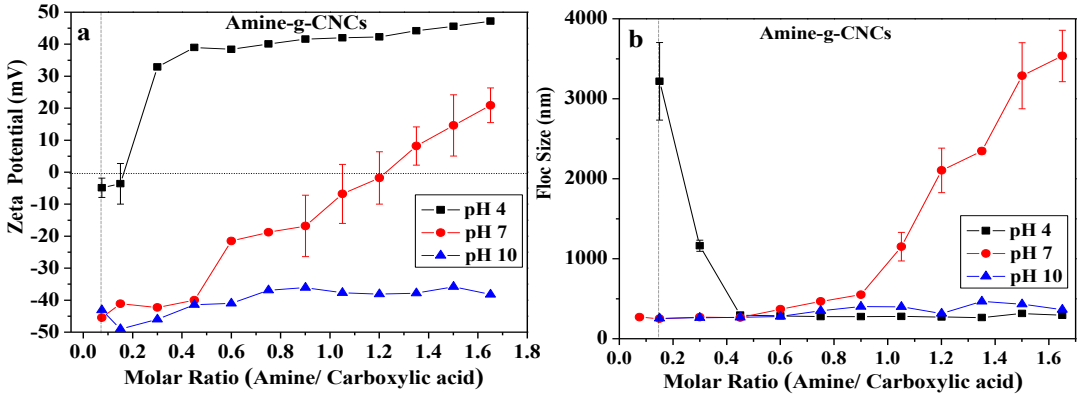

Figure 2.11 Floc properties under three different pHs from Amine-g-CNCs flocculants (a) Zeta potential value (b) floc size.

2.3.2.3 Amine type effect

In order to compare the flocculation behaviour and capability among different amine types, optimal dosage, flocculation efficiency and flocs size of cationic flocculants have been summarized in Table 2.1. The basicity of amine type as discussed before, follow an order of pyridine amine < tertiary amine < primary amine. Further insights can be drawn from the information for comparison.

Among these three types of amine, at pH=4 and pH=7, primary amine from the amine-g-CNCs gave the best flocculation performance based on the lowest optimal mixing ratio, which was explained by the charge neutralization mechanism resulting from the stronger intermolecular force.[75] However, the strongest interaction also resulted in the narrowest flocculation window due a more significant charge reversion that induced the re-stabilization of the latex particle. This

re-stabilization can also be observed at high amount of PDMA-g-CNCs with tertiary amine group, not for the weakest base of pyridine group in P4VP-g-CNCs. It was also notable that, pyridine amine, which was weaker than tertiary amine, in contrast, had a lower optimum ratio as evident from Table 2.1 at pH 4. This is ascribed to "bridging effect" dominated the flocculation pathway in P4VP-g-CNCs with latex particles, so that flocculation efficiency was less dependent on charge neutralizing capability. Most negative flocs charge and largest flocs size from P4VP-g-CNCs at te optimum mixing ratio were further confirmed this finding.

Table 2.1 The optimal dosage and corresponding flocculation efficiency of cationic flocculants.

Flocculants		PDMA-g-CNCs	P4VP-g-CNCs	Amine-g-CNCs
pH 4	Ratio $_{optimal}$	0.26	0.15	0.07
	Floccualtion window	0.26 to 1.05	0.15 to 0.30	0.07 to 0.15
	FE (%)	97.80 to 98.2	97.6 to 97.7	98.2 to 100
	Floc size range	1043 to 1468 nm	614 to 6112 nm	1193 to 3125 nm
pH 7	Ratio $_{optimal}$	1.66	1.66	1.35
	Floccualtion window	No	No	1.35 to 1.66
	FE (%)	80.5	77.3	95.1 to 100
	Floc size range	3095 nm	4938 nm	2067 to 3561 nm
pH 10	Ratio $_{optimal}$	1.66	N-A	N-A
	Floccualtion window	No		
	FE (%)	80.5	4.1	11.0
	Floc size range	1097 nm	262 nm	444 nm

a Ratio $_{optimal}$ is the optimal mixing ratio when the highest removing efficiency occurs
b Flocculaiton window is over the certain range the highest moving efficiency restained
c FE is abbreviation for flocculaiton efficiency which calcualte through Uv-vis transmittance

At pH=10, when all the various types of functional group became protonated and the polymer chain collapsed, the PDMA-g-CNCs still possessed flocculation capability, which produced fairly large floc of 1000 nm, where the hydrogen bond was assumed to be the driving force for inter-molecular attraction followed by van der Waals forces to induce floc agglomeration.

2.4 Conclusions

A series of novel cationic bio-flocculants based on CNCs have been successfully prepared and characterized using various techniques. The results demonstrated that PDMA, P4VP and polyamine were successfully grafted from the CNC surface. Flocculation tests at various pH levels indicated that these modified CNCs are effective bio-flocculants for colloidal suspension.

The change in the conformation of amine group and polymer structure determined the flocculation efficiency and the dominant flocculation pathway. At pH=4, charge neutralization was suggested for amine-g-CNCs and PDMA-g-CNCs and re-stablization occurred at higher mixing ratio. Bridging effect was more obvious for P4VP that produced relatively large size flocs.

The greatest interaction strength from amine-g-CNCs produced the best flocculation performance that corresponded to the lowest optimal mixing ratio of pH=4 and a wider flocculation window at pH=7. On the other hand, when the flocculation occurred through ionic interaction between functional groups on PV4P-g-CNCs and amine-g-CNCs, pH played an important role. This can been seen from the weakest amine and strongest amine, i.e. no flocculation phenomena was observed in alkali condition when the amine groups lost their functionality. The presence of carbonyl group from PDMA polymer chain induced potential hydrogen bonding that contributed to the aggregation of the latex particles.

Nevertheless, floc density and space filling ability still needs to be further investigated to obtain a comprehensive conclusion of the performance of these bio-flocculants.

Chapter 3. GTMAC-Chitosan Modified Cellulose Nanocrystals (CNCs), a Novel Polymer/Nanoparticle Flocculants for Bentonite Clay Flocculation

3.1 Introduction

The basic classification of various coagulants and flocculants can be classified as inorganic metals salt, organic synthetic polymers, and polymer-grafted bio-flocculants. The main disadvantage of polymer containing flocculants is that polymer chains undergoing chain conformation, and loose its secondary structure as well as functionality in a high ionic strength/alkaline medium,[19,46,114]. This hinders their effective contact between flocculants and suspended particulates and ultimately limits its universal application.

Various novel polymer systems including dual-polymer system and microparticle/polymer flocculants have received greated acceptance. Dual systems include polyampholytes and polyelectrolyte complex (PEC), a polyampholyte carry both positive and negative charges that are covalently bonded to the polymer backbone. The intermolecular associations of polycation and polanion form the PEC, which are designed to act as polyampholytes,[124,178], consisting of merely physical mixtures of positively and negatively charged molecules. These dual system polymeric flocculants with varied molecular architecture and functional groups are capable of producing robust, dense and compressible flocs under different conditions. Microparticle/polymer flocculants have emerged as novel systems that are created based on either organic/inorganic or organic/organic

hybrids. For instance, $Al(OH)_3$-polyacryamide (PAM) hybrids have a cationic core of an $Al(OH)_3$ colloid functioning through electrostatic interactions and adsorption between the polyacrylamide chain arms and kaolin particles via hydrogen bonds.[66] Another example is chitosan with montmorillonite, which displayed a synergistic effect and was less dependent on the pH and composition of liquid medium. Cationic starch cross-linked with chitosan (CATCS), which can be regarded as a biodegradable organic/organic hybrid, possesses improved flocculation properties over unmodified cationic starch and chitosan. The goal of dual flocculation systems is to have synergistic effects from both components of the hybrid materials, consisting of an apparent high molecular weight, extensive macromolecule configurations and as well as good bridging effects. Characteristics such as fast settling velocity, good dewatering ability and dense packing ability to prevent residual bonded water are important features of excellent flocculants.[179–181]

These novel flocculants are promising system for optimizing floc properties that would facilitate easy solid-liquid phase separation and yield major cost and energy savings in large scale operation. Chitosan, a material derived from natural sources, is a linear copolymer of D-glucoamine and N-acetyl-D-glucoamine produced by deacetylation of chitin, and is one of the most outstanding candidates under the category of natural flocculants[128]. Its intrinsic positive charges from the primary amine groups along the polysaccharide backbone makes it an effective coagulant/flocculant. In fact, it has been successfully applied for the treatment of pulp mill wastewater,[129] papermaking-processing effluent,[130] dye,[143] mineral,[169] chemical laden sewage,[146], as well as the removal of organic compounds,[131] inorganic nutrients,[74] and bacteria from aquaculture

wastewaters.

Cellulose nanocrystals (CNCs) are rod like nanoparticles derived from cellulose with width of 5-20 nm and length of 200-400 nm. These nanoparticles are produced via the acid hydrolysis of cellulose, a process that removes the amorphous regions of cellulose fibers to yield crystalline rods. CNCs are easy to fabricate, and they are biocompatible, biodegradable, and are regarded as having moderate thermal and chemical stability.[167] Their high aspect ratio, crystalline hydrophobic backbone, simple surface modification would advance its application as flocculants. It is very valuable to explore the flocculation capability of these well-defined CNCs. Here, an attractive material was produced through the combination between CNCs and chitosan. Chitosan was initially modified with glycidyl trimethylammonium chloride (GTAMC) in order to enhance its solubility over a wide pH range. Schiff base reactions between the primary amine groups on chitosan and aldehyde groups from oxidized CNCs yielded a polymer/nanoparticle flocculant system. The flocculation behavior for both GTMAC-Chitosan and CNCs incorporated chitosan were investigated by varying the dosage over a wide range of pHs. Comparisons were made in terms of flocculation mechanism and floc morphology to elucidate the potential function of introducing CNCs in flocculants. Other than the common flocculation mechanisms by charge neutralization, bridging effect, or patch attraction, attaching GTMAC-Chitosan onto CNCs surface caused the polymer chains to lose their flexibility and high charge density, which would only function as binding sites in the initial stage of floc formation. The high aspect ratio of CNCs provided large anchoring area for particle collision, which enhanced the floc formation and agglomeration. As

expected, this novel flocculants displayed a clear increase on floc size. The floc morphology parameter, such as the shape factor and fractal dimension value, demonstrated that smaller flocs from GTMAC-Chitosan were elliptical in shape. Likewise, larger flocs derived from GTMAC-Chitosan/A-CNCs displayed a spherical shape, and a high fractal dimension pointing to its excellent space filling capacity.

3.2 Experiment

3.2.1Materials

Cellulose nanocrystals hydrolyzed from wood pulp with an average charge density of 0.26 mmol/g were provided by CelluForce Inc. All reagents were purchased from Sigma-Aldrich unless otherwise stated. Chitosan, (low molecular weight, deacetylated ≥75%), Glycidyl trimethylammonium chloride (GTMAC), sodium periodate ($NaIO_4$), silver (I) oxide (Ag_2O), Acetone (≥ 99.5%). .Potassium bromide (KBr), Acetic acid (HAC), silver nitrate ($AgNO_3$), Hydrochloride acid (HCl 1M) solution and sodium hydroxide (NaOH 1M) standard solutions were used as received. Water (≥ 18 MΩ cm) used in all procedures was filtered through a Millipore Mill-A purification System.

3.2.2 Preparation of glycidyl trimethylammonium chloride-chitosan (G-Chitosan)

G-Chitosan was synthesized by a one step as shown in Scheme 3.1. 4.0 g of chitosan was dispersed in 100 ml of 1.0% (w/w) HAC aqueous solution, followed by homogenization (IKA T25) for three minutes to ensure the complete dispersion of the chitosan polymer. The mixture was transferred into a round bottom flask, and GTMAC monomer was introduced at a 1:1 molar ratio

(glucosamine/GTMAC) and stirred for 4 hours at 50 ^{O}C. Then, acetone was added to the mixture at a 3:1 volume ratio, followed by 3 vortex/centrifugation cycles to remove unreacted GTMAC. The purified G-Chitosan was then dispersed in water and dialyzed (12,000 Da MW cutoff) extensively against deionized water for one week until the measured water conductivity remained constant. The sample was freeze-dried to yield a solid product.

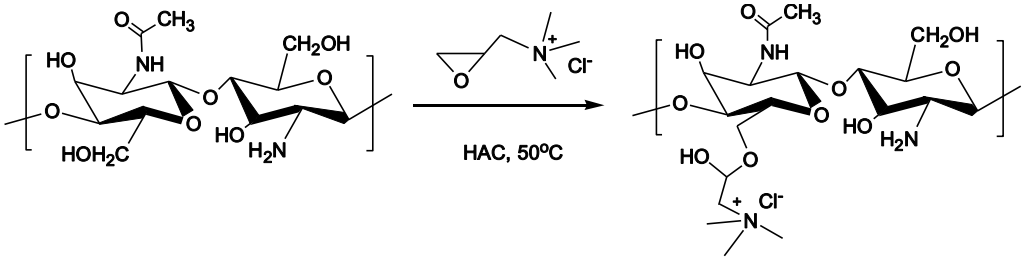

Scheme 3.1 Synthesis of GTMAC functionalized chitosan.

3.2.3 Periodate oxidation of CNCs

1.0 g of CNCs was dispersed in 100.0 ml of 0.05 M sodium periodate aqueous solution in a 250 ml beaker equipped with a magnetic stirrer. The mixture was gently stirred at room temperature (25^{o}C) overnight in the dark, and excess periodate was consumed with the addition of ethylene glycol and the dispersion was centrifuged once to remove dissolved and unreacted chemicals The modified CNCs were re-dispersed in water through vortexing and the final solution was extensively dialyzed (M_W cutoff of 12 000 Da) against deionized water for at least one week until the measured conductivity of the water remained constant. The purified solution was concentrated and freeze-dried for further evaluation.

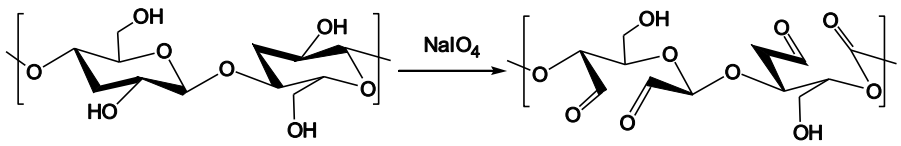

Scheme 3.2 Periodate oxidation of CNCs.

3.2.4 Preparation of GTMAC-Chitosan modified Aldehyde-CNCs

G-Chitosan/A-CNCs were prepared via the Schiff base reaction. 20.0 ml of 7.5 g/L aldehyde CNCs were prepared as the bulk solution, 30.0 ml of 3.4 g/L GTMAC-Chitosan solution was gradually added dropwise into A-CNCs in order to avoid undesirable particle and polymer aggregation. The mixture was gently agitated in a sonication bath, was kept stirring for several hours to ensure the polymer was uniformly distributed on the CNCs surface. The sample was freeze-dried and tested for their flocculation behaviour.

3.2.5 Characterization of flocculants

FTIR spectra were recorded for the determination of new functional groups by comparing the polysaccharide before and after modification. The spectra were acquired at room temperature using the Bruker Tensor 27 spectrometer FT-IR spectrometer with a resolution of $4cm^{-1}$ and 64 scan between 400 cm^{-1} to 4000 cm^{-1}. Test pellets were prepared by grinding and compress approximately 1% (w/w) of the sample: CNCs, Aldehyde-CNCs (A-CNCs) in potassium bromide (KBr).

Determination of degree of substitution (DS) of G-Chitosan: The DS is defined as the molar ratio of bonded GTMAC per mole of glucosamine calculated from the original mass of chitosan and its degree of deacetylation (DD).[182] The DS was measured by conductometric titration using a Metrohm 809 Titrando autotitration to titrate chloride ions. The formula to determine the DS of G-Chitosan is described by Equation 3. 1

$$DS = \frac{V \times C/1000}{V \times C/1000 + (W - V \times C \times 314/1000)/162} \times \frac{1}{DD} \times 100\% \qquad (3.1)$$

V (ml) is volume of silver nitrite ($AgNO_3$) calculated from the inflection point where the conductivity of the solution is lowest with the stepwise addition of $AgNO_3$ solution. C (mol/l) is concentration of $AgNO_3$ solution, W (g) is the mass of G-Chitosan, and DD is the degree of deacetylation of chitosan. Quaternary glucosamine has a molar mass of 314.0g/mol, and glucosamine molar mass is 162.0 g/mol.

Determination of aldehyde content: The number of aldehyde groups on CNC was also quantified via conductometric titration after selectively oxidizing the aldehyde groups to carboxylic acid groups using silver (I) oxide as report before.[183] In brief, 25.0 mg of Aldehyde-CNC was added into 10 ml of aqueous solution containing 96.6 mg silver (I) oxide and 12.4 mg of sodium hydroxide and was allowed to stir overnight to ensure all aldehyde groups were converted to carboxylic groups. Half of the total oxidized reaction mixture was diluted in 40.0 ml water to be used for conductometric titration.

The ξ-potential (ZP) of each sample was measured at room temperature using a Malvern Nano-ZS90 Zetasizer. The concentration of the samples was 0.1% (w/w). A total of three measurements were acquired for each sample, and the value was obtained by averaging the measurements.

The morphologies of flocculant samples were evaluated using a Philips CM 10 transmission electron microscopy (TEM) with a 60 kV accelerating voltage. TEM sample were prepared by spraying 25μm of a 0.05% w/w sample solution onto a carbon-coated copper grid followed by

drying under ambient conditions.

3.2.6 Flocculation experiments

Flocculation procedure

Bentonite clay (1.0 g) was added into 1 L distilled water and homogenized (IKA T25) for 20 minutes under stirring at 400 rpm to ensure the complete dispersion of clay particles. HCl and NaOH standard solutions were used to modify the pH of the mediums. G-Chitosan and G-Chitosan/A-CNCs flocculants stock solution of 2.0 g/L were prepared in the distilled water before each flocculation test. The flocculation tests were conducted in 7 ml glass vials at room temperature. Rapid mixing at 200 rpm for 2 minutes allowed for the formation of floc, followed by 45 minutes of settling before collecting the supernatant turbidity and ZP analysis. The residual turbidity is expressed in Equation 3. 2.

$$\text{Residual Turbidity (RT)}\% = \frac{T_{treated}}{T_{blank}} \times 100\% \qquad (3.2)$$

Where $T_{treated}$ and T_{blank} are the turbidity of clay suspension with and without flocculants treatment respectively. The turbidity was converted from the absorbance obtained at λ=500 nm using UV-Vis Spectrophotometry.

Floc surface charge

The ξ-potential (ZP) of each floc sample was measured at room temperature using a Malvern Nano-ZS90 Zetasizer. After mixing, the floc was charged and diluted with 1:5 ratio to prepare a suspension. Then it was tested for surface charge properties and the value were calculated.

Floc size and fractal dimension

The floc morphology was visualized using an inverted optical microscope (Carl Zeiss Axio Observer. Z1m) equipped with a CCD camera (Carl Zeiss Axio Cam 1Cm1). Floc sample droplets were placed directly onto a glass slide and captured under 5−50× magnification. A and *l* were derived from the photos to spot 50 to 100 floc segments, and the results were produced automatically by the software. The average value was taken as the A and *l* for each sample.

The projected area diameter was calculated as Equation 3. 3

$$D = 2\sqrt{\frac{A}{\pi}} \qquad (3.3)$$

Where D is projected area diameter, A is objected area.

Fractal dimensions relate the aggregate size to one dimension perimeter, two dimension area as well three dimension light scattering intensity. Here we can use the optical microscopy to determine the two dimensions are as described in Equation 3. 4

$$\mathrm{A} \propto l^{D_2} \qquad (3.4)$$

D_2 means object area increases to the power of the object length increases and D_2 always smaller than 2, based on two-dimensional capacity, particle area increased slower than the square of length scale.

3.3. Results and discussion

3.3.1 Flocculants characterization

FT-IR has been utilized to characterize the chemical linkage of modified CNCs flocculants. Figure 3.1 presented to FT-IR spectrum of CNCs, A-CNCs. A characteristic band of A-CNCs appeared in the 1640 cm^{-1} region was ascribed to C=O of aldehyde group which may overlap with

primary hydroxyl group of pristine CNCs, a shoulder peak appeared at 2850 cm^{-1} because C-H stretching from carboxyl group was more evident for the presence of aldehyde group.

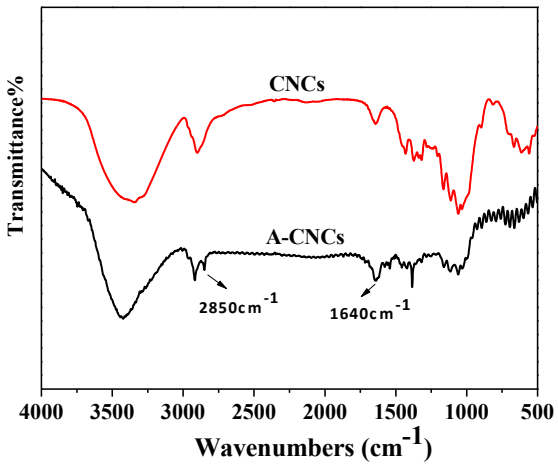

Figure 3.1 FT-IR spectra of CNCs, A-CNCs.

The degree of substitution of GTMAC-Chitosan was calculated from the conductometric titration of chloride counterions using silver nitrate. The titration data for G-Chitosan is presented in Figure 2.1, showing two stages that were delineated by the conductivity inflection point. The first stage shows a slight linear decreased due to silver cations binding with chloride counterions of quaternary ammonium group to form a silver chloride precipitate. The second stage displayed a sharp increase resulting in the dissociation of silver nitrate to form free silver cations and nitrate anions, which occurred only after the consumption of all chloride counterions. The point of intersection corresponded to the volume of sliver nitrate consumed, which provided information on the DS of GTMAC on Chitosan. The amounts of carboxylic acid groups present on the CNCs from aldehyde oxidation could be quantified via conductometric titration using HCl standard titrant. Dosing HCl into a solution of modified CNCs will initially neutralize free hydroxide ions, causing a decrease in

the pH and conductivity in the first stage. When the pH approached the pKa of the carboxylic acid functional group, the OH^- began to react with functional groups on the CNCs surface resulting in the deprotonation of the carboxylic acids. This caused the conductivity curve to approach a plateau region until all the functional groups on CNCs were completely deprotonated, which signified the end of the second stage. Continual dosage of HCl titrant caused a fast increase in conductivity resulting from the dissociation of titrant, which constituted the third stage. The region between the 2 equivalent lines shown in Figure 3.2（b）corresponds to the amounts of carboxylic acid groups.

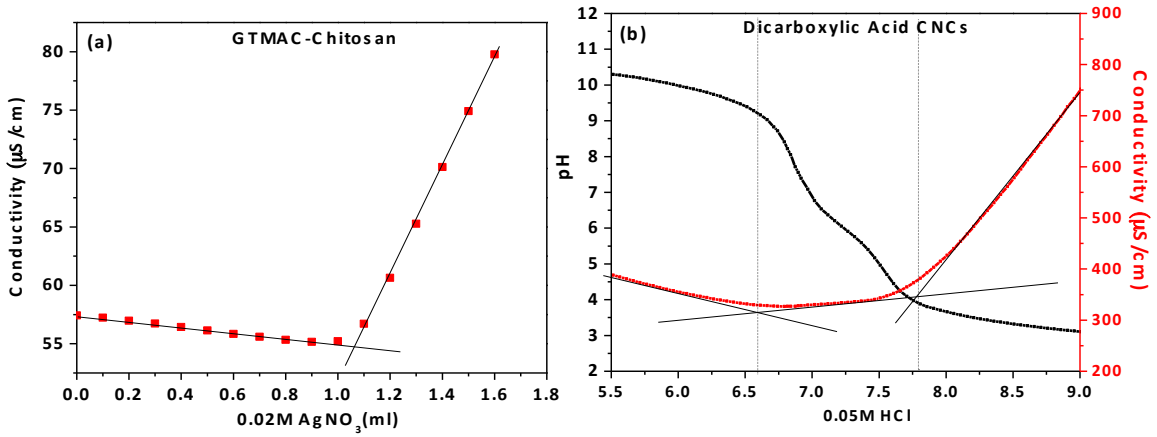

Figure 3.2 Conductomatric titration of (a) GTMAC-Chitosan and (b) Dicarboxylic acid CNCs.

As described previously, G-Chitosan polymer displayed enhanced solubility, which is beneficial for the preparation over a wide pH range. The introduction of quaternary ammonium groups possessing greater hydration capacity reduced the intermolecular and intramolecular hydrogen bonding between adjacent chitosan chains; enabling the modified chitosan to act as a water-soluble cationic polyelectrolyte.[184] When the modified chitosan was incorporated onto the A-CNCs surface, the chitosan polymer chains wrap around the CNC rods or connect adjacent

particles, while all segments are still solubilized in water. These chitosan-based flocculants at various pH levels were tested and they are shown in the figure of particle size and solubility of GTMAC-Chitosan/A-CNCs flocculants over the operating pH.

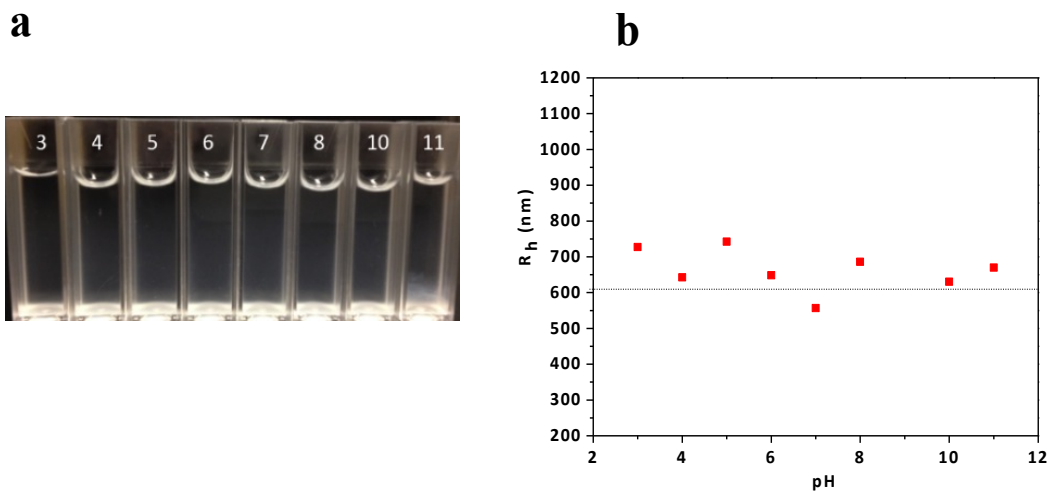

Figure 3.3 GTMAC-Chitosan/A-CNCs flocculants (a) solubility; (b) particle size.

A 1g/L of GTMAC-Chitosan-g-A-CNCs flocculants were prepared and the dispersibility and particle size of flocculants were determined and shown in Figure 3.3. It is evident Figure 3.3(a), that the dispersions were transparent solution between pH of 3 to 10, and only when pH exceeded 11, G-Chitosan/A-CNCs aggregated and settled to the bottom of the cuvette.

In order to elucidate the flocculation performance of G-Chitosan and G-Chitosan/A-CNCs under a series of dosage, three different concentrations of bulk clay suspension was prepared by varying the flocculants dosage at pH of 7. It can be seen from Fig. 3.4 (a), 0.5g/L. 1.0 g/L and 1.5 g/L of clay gave similar trend in terms of residual turbidity, the optimal dosage occurred around 50 mg/L and reversibility occurred soon after the optimum was achieved. Due to the strong electrostatic interaction of polymer flocculants with clay particle, excess flocculants can restabilize the system

and decrease the turbidity resulting in a reduced efficiency. However, in all three concentrations with G-Chitosan/A-CNCs flocculants, the residual turbidity gradually decreased with the addition of more flocculants and the optimal residual turbidity was maintained after the clay particle has been settled to the bottom of the cuvette. No definite conclusion could be draw over these three different concentrations possibly because the concentration value were close to each other, nevertheless, it provided a qualitatively recognition of the flocculation behavior of both flocculants, and 1.0 g/L was selected as the clay bulk concentration for further studies.

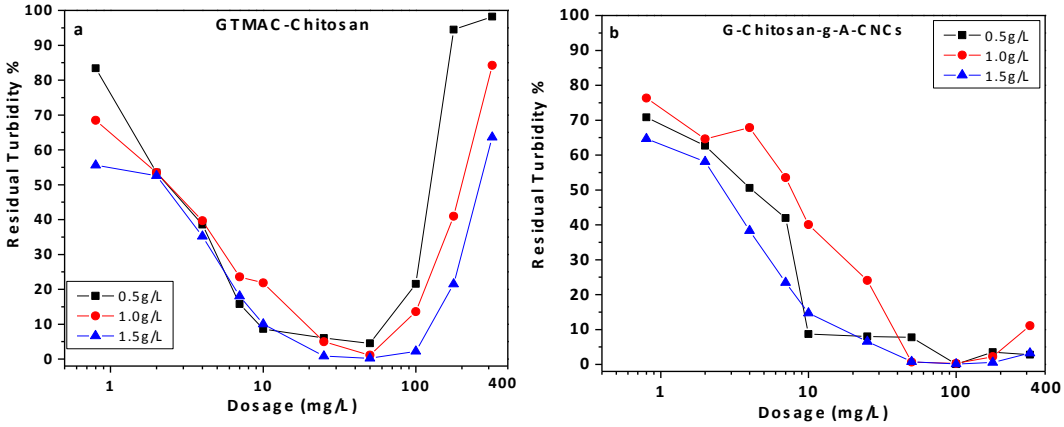

Figure 3.4 Flocculation characteristics of three different bulk clay concentrations with varied flocculants dosage (mg/L) (a) GTMA-Chitosan; (b) G-Chitosan-g-A-CNCs

As expected, G-Chitosan/A-CNCs flocculants demonstrated excellent dispersibility in aqueous solution over a wide pH range of 3 to 10 and the flocculants size was in the range of 600 nm.

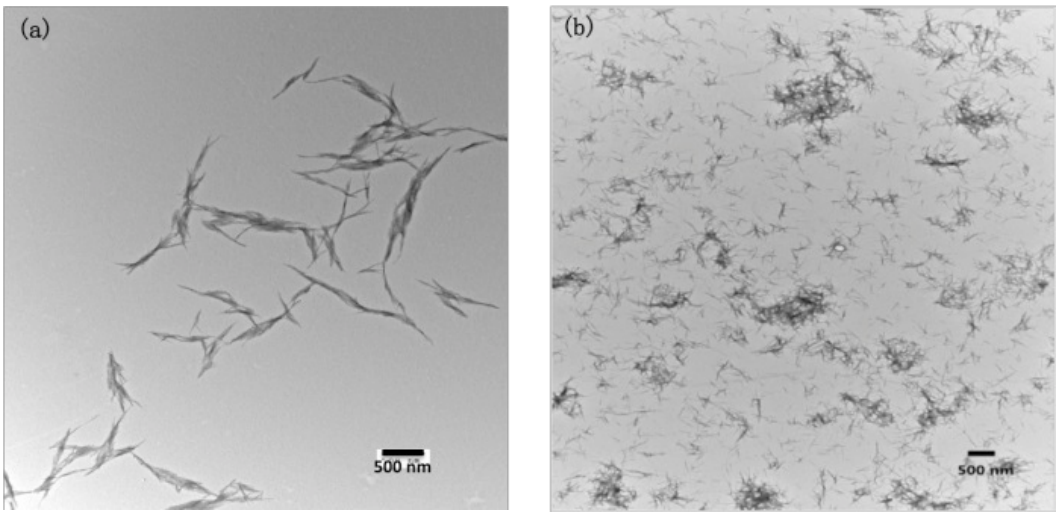

Figure 3.5 TEM image of (a) pristine CNCs (b) G-Chitosan/A-CNCs.

The morphology of pristine CNCs and G-Chitosan/A-CNCs is shown in Figure 3.5. Pristine CNCs comprised of a thin rod with length of around 400 nm. However, the length of G-Chitosan/A-CNCs was decreased even though the rod-like structure was preserved, and some aggregation was observed. One possible reason could be the periodate oxidation step may exfoliate the surface layer of CNCs, and the insertion of an electronegative aldehyde group increased the inter-particle repulsion and resulted in a more dispersed system.[185] Following the addition of chitosan, the polymer chains wrap around the A-CNC nanoparticles to yield another microstructure, as evident for the G-Chitosan/A-CNCs flocculants shown in Figure 3.5b.

The zeta potential of bentonite clay, G-Chitosan and G-Chitosan/A-CNCs was also measured and displayed in Figure 3.6. The phyllosilicate of clay comprised of a continuous tetrahedral and octahedral sheet and the universal formal $Al_2Si_2O_5(OH)_4$.[186] The negative surface charge of the clay came from the hydrolysis of hydroxyl groups present on either silica-like or alumina-like planes. The broken edges of the clay nanoparticles containing the more reactive sites, are highly

pH-dependent.[187] When the pH exceeded the isoelectric point (IEP) of aluminol (IEP) and silanol (IEP), more positive groups were converted into negative charges, which ultimately caused the clay to become more negatively charged with increasing pH.[188] For both G-Chitosan and G-Chitosan/A-CNCs, the deprotonation of surface primary amine groups (pKa of 7.5) with increasing pH led to a lower net positive charge, while still maintained a slight positive charge under alkaline conditions due to the quaternary ammonium groups. The covalent bond formation between amine and aldehyde groups resulted in lower positive charges on the G-Chitosan/A-CNCs. However, at a pH above 7, the primary amine groups become deprotonated and they no longer contribute to the net charge.

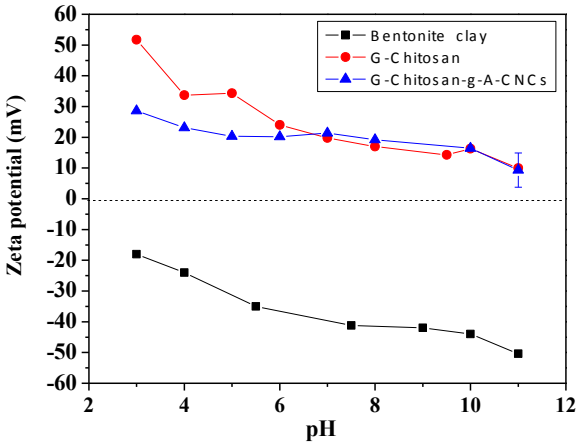

Figure 3.6 ξ-potential value of bentonite clay, G-Chitosan and G-Chitosan/A-CNCs flocculants over pH range from 3 to 11.

3.3.2 Evaluation of the optimal dosage of the flocculants at various pH levels

3.3.2.1 Effect of pH

A variety of external parameters can affect the flocculation efficiency of flocculants; pH and

dosage were chosen as primary ones to study. Turbidity and zeta potential measurements were conducted to evaluate the effectiveness of these two flocculants. Plots (a), (b) and (c) in Figure 3.7 demonstrate the flocculation behavior of GTMAC-Chitosan at various pHs.

From the turbidity-dosage profile at pH 4, 7 and 10, the general trend was that the residual turbidity decreased with the addition of GTAMC-Chitosan, until it reached the optimal dosage (OD). With the continual dosing of flocculants, the solution became turbid again. Optimal dosages under pH 4 and 7 were 10 mg/L and 50 mg/L respectively. Further increase of the pH to 10, an optimum residual turbidity was maintained; G-Chitosan exhibited better performance that was proven by a wider flocculation window. It was believed that the conformation of the flocculant molecule has a significant impact on its performance. At pH 4 the polymer was in an extended state, and high charge density enabled the polymer to display a more favorable architecture. The effect of intra-chain electrostatic repulsion facilitated a high degree of contact between the bentonite clay and G-Chitosan, which was beneficial for the flocculation efficiency and resulted in the lowest OD. Residual turbidity was restored with a further increase in flocculants content, and an excess polymer would reduce the flocculation efficiency. When the pH was increased to 7, the polymer was partially deprotonated, and the diminished charge density reduced the hydrodynamic radius of the G-Chitosan. The number of active site declined, combined with a coiled polymer chain structure resulted in a higher OD, resulting in the flocculation of the same amount of bentonite clay particles. Re-dispersion could also be achieved at pH 7, as the residual turbidity instantly increased right after OD. However, under alkaline conditions, GTMAC-Chitosan was proven to have a wider

flocculation window and demonstrated decreased sensitivity to dosage. Considering that all of the amine functional groups were deprotonated, the residual surface charge of the G-Chitosan came from the GTMAC portion of the quaternary ammonium ion, whereas, the OD was kept and extended from 50 mg/L to 100 mg/L where the lowest residual turbidity was retained.

In order to explain the flocculation process, more information has to be extracted from the ZP-dosage profile. All of the pH levels exhibited a negative to positive surface charge transition. One flocculation mechanism, charge neutralization, is defined when the OD occurs when the flocculants/particle complex becomes electrically neutral. The interaction between the two oppositely charged systems promoted the polymer to adsorb onto the bentonite clay surface, reducing the electrical double layer around the clay colloidal particle and destabilizing the particle.[189] It is known that polymers possessing a high charge density will be attracted to the colloidal surface and form an "adsorption layer". However, when the flocculants amount exceeds the OD, the built-up polymer layer will lead to charge reversion,[190] which explained the further increasing of residual turbidity at higher polymer flocculants content.

At pH 7, it was thought that the formation of flocs was caused by a "bridging effect" due to the reduction of polymer charge density, which would cause the polymer to attach onto clay particle surface in "loops and tails" fashion. Clay particles were linked or bridged together by different binding sites on the polymer backbone, which in turn resulted in a higher OD and larger flocs size. The bridging effect became more evident in alkaline conditions resulting in a more negatively charged flocs at OD. When all amine groups were deprotonated, the polymer structure collapsed

and stabilized by the residual positively charges of the GTMAC functional groups. In this condition, the polymers had the ability to "patch" the clay surface on multiple sites. The dipolar attraction existed between polymer-attached regions and patch-free regions of adjacent negatively charged clay, which induced the particles to form large flocs. This would result in an overall larger negative charge at OD.[143]

Fig. 3.7 (e) (f) and (g) display the flocculation performance of G-Chitosan/A-CNCs at pH 4, 7 and 10 respectively. The flocculation behavior by G-Chitosan was optimal, where the OD was 10 mg/L, 50 mg/L and 177 mg/L at pH 4, 7 and 10, respectively. Residual turbidity gradually decreased with flocculants dosing and the ZP remained constant and started to increase when the flocculation dosage approached the OD.

As expected, after the polymer was grafted onto the CNC surface, less amine groups were available to interact with the clay surface, and the chain flexibility was also limited. In this case, since the surface charge of the flocs was constant as the residual turbidity continued to decrease, it can be reasoned that the flocculation no longer followed the charge neutralization pathway. The polymer was assumed to promote charge attraction in the initial stages of the floc formation; however, the impact of the polymer became less significant once it was grafted onto the CNCs surface. The charge attraction initiated bridging between G-Chitosan/A-CNCs with clay particles to produce microflocs. Upon agitation, microflocs would further aggregate after encountering external shear forces to form macroflocs and consequently precipitate out of the solution.

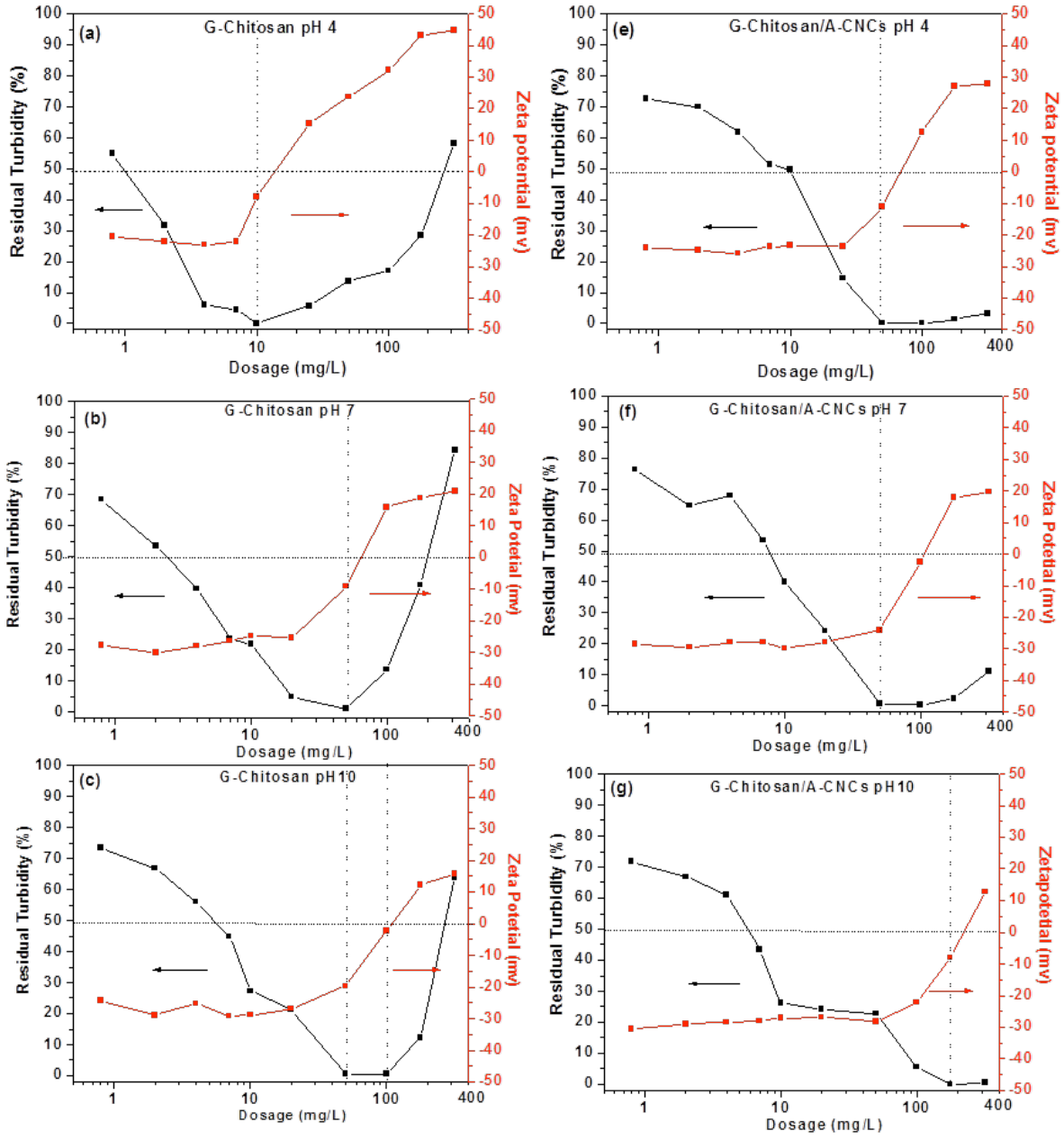

Figure 3.7 Residual turbidity and ZP by adding G-Chitosan and G-Chitosan/A-CNCs, respectively as a function of dosage (mg/L) under pH 4, 7 and 10 respectively: (a), (b) and (c) are the G-Chitosan sample; (e), (f) and (g) are the G-Chitosan/A-CNCs sample.

It was found that the same OD was required at pH 4 and 7, which suggests that the pH was not a

significant factor at acidic/neutral conditions and that the influence of the polymer was diminished. When all of the amine groups were protonated at pH 10, the active sites decreased significantly which impaired the flocculation efficiency and caused OD to shift to a higher value. Over the entire range of flocculant dosage, no restabilization occurred, and the lowest residual turbidity was maintained after the OD.

3.3.3 Floc size: Projected area diameter D (μm)

Typically when referring to floc size, the usual convention is to calculate the equivalent diameter of a circle possessing the same corss sectional area of the floc as observed in micrographs. By utilizing this standardized measurement, comparisons can be made between irregular structures. The dimension based on a two-dimensional image is known as a statistical diameter, and they are acceptable when sufficient measurements are made.[181] Here we chose one of most common equivalent diameters to characterize the floc aggregates, the projected area diameter according to Equation 3.1 by observing 50 to 100 floc segments and taking the average value as summarized in the figures below. Floc sizes at three pHs for GTMAC-Chitosan and GTMAC-Chitosan/A-CNCs were displayed in Figure 3.8 (a) and (b) respectively. As evident from (a) in Figure 3.8, the floc size increased with the addition of G-Chitosan. The maximum floc size at pH 4, 7 and 10 were 72 μm, 141μm and 332 μm respectivily. It was found that the largest flocs occurred at pH 10, and this behavior was also observed for the chitosan polymer, where the flocculation mechanism was attributed to bridging effect, which produced a larger floc size.[191]

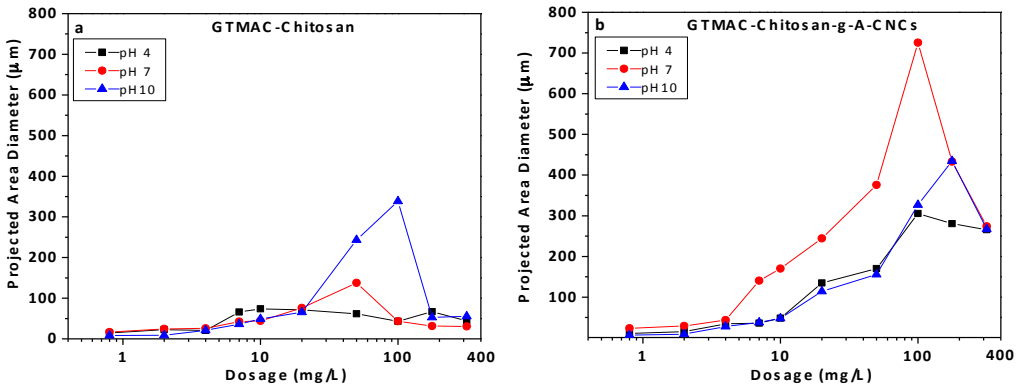

Figure 3.8 Projected area diameter of floc as a function of flocculants dosage (mg/L) (a) G-Chitosan; (b) G-Chitosan/A-CNCs.

The protonation of amine functional groups under alkaline condition caused the polymer chain structure to collaspe, hence more flocculant were required to achieve to produce a larger floc size. It is commonly accepted that a larger floc dimension with broader flocculation window was much more desirable for polymer flocculants, especially under alkaline conditions where amine functionalized flocculants lose their charge characteristics. Here the results showed the quaternary ammonion modification not only enhanced the chitosan solubility, but also maintained its flocculation effectiveness.

Similar results were observed from Fig. 3.8 (b) with G-Chitosan/A-CNCs flocculants, where the floc size peak occurred at 307µm, 717µm and 436µm, however the flocculant amount was not identical with OD, and pH 7 gave the largest floc size. By incorporating Chitosan onto the CNCs surface, charge availablity and chain length will be limited to a certain degree. Instead of being a flat layer, the coverage of polymer/microparticles on the clay particles surface was assumed to be

irregular. Through this patching/bridging process, the resulting floc became larger. However, when operating at pH 10 the amount of active binding sites was reduced, and consequently the polymers ability to flocculate the clay particles was reduced.

3.3.4 Flocs shape and fractal dimension

Static flocs were observed using microscopy to gain an idea of the floc shape. In order to ensure the exact floc was observed, the sample preparation must minimize the breakage or changes in the floc, as well as preventing further aggregation.

Figure 3.9 displays the floc morphology with varied G-Chitosan flocculant dosage at pH 4, 7 and 10. Three flocculant dosages, (at which floc morphology was more appreciable), were chosen to investigate the floc properties, floc images at the OD have highlighted in a red frame. The results were identical with the equivalent diameter, which was calculated from standardizing the irregular form as a sphere or circle. Both the flocs at pH 7 and 10 were visually larger than those observed at pH 4, and the flocs at the OD had the largest dimension and appeared to be more compact. The flocs at the OD were found to be more elliptical, yielding a rod-shaped outline at pH 4 and 7. This was likely caused by sufficient surface charge allowing the particles to maximize their separation distance, resulting in a chain-like morphology.[192] However, this structure disintegrated at pH 10, becoming a more porous and loose structure. The irregular, fuzzy frame of the flocs further supported this claim. It was found that when the flocculation amount was lower and higher than the OD, the floc morphology would be loose and smaller due to the external charge repulsion between microflocs that reduced the aggregation of the flocs.

Some aggregate morphology parameters have been applied to quantitively describes the floc geometry. We applied a dimensionless shape factor, F, which is derived from the ratio between the greatest length "*L*" of dynamic radius-equivalent ellipse as shown by the green line in the Figure 3.10, and the mean projected diameter shown in Figure 3.10 as "D_c ", which was indicated by the red line embedded in the sphere, so F= L/D_c. The universal shape was assigned under each F range. Within Figure 3.10, F values were more than 2 for flocs observed at pH 4 and 7 at the OD, whereas it decreased to 1.5 for pH 10 at the OD.[193] The "F" values calculated by the above procedure were in agreement with our observations from the microscopic image. "F" values larger than 2 showed more irregular shape and had a more elliptical outline, where the "F" values close to unity tended be uniform and spherical. Nevertheless, those whose silhouettes showed many inlets and voids may also be included, due to the limitation of two-dimensional structure images. The exploration of floc packing density may be determined from the fractal dimension calculation, which will be discussed later.

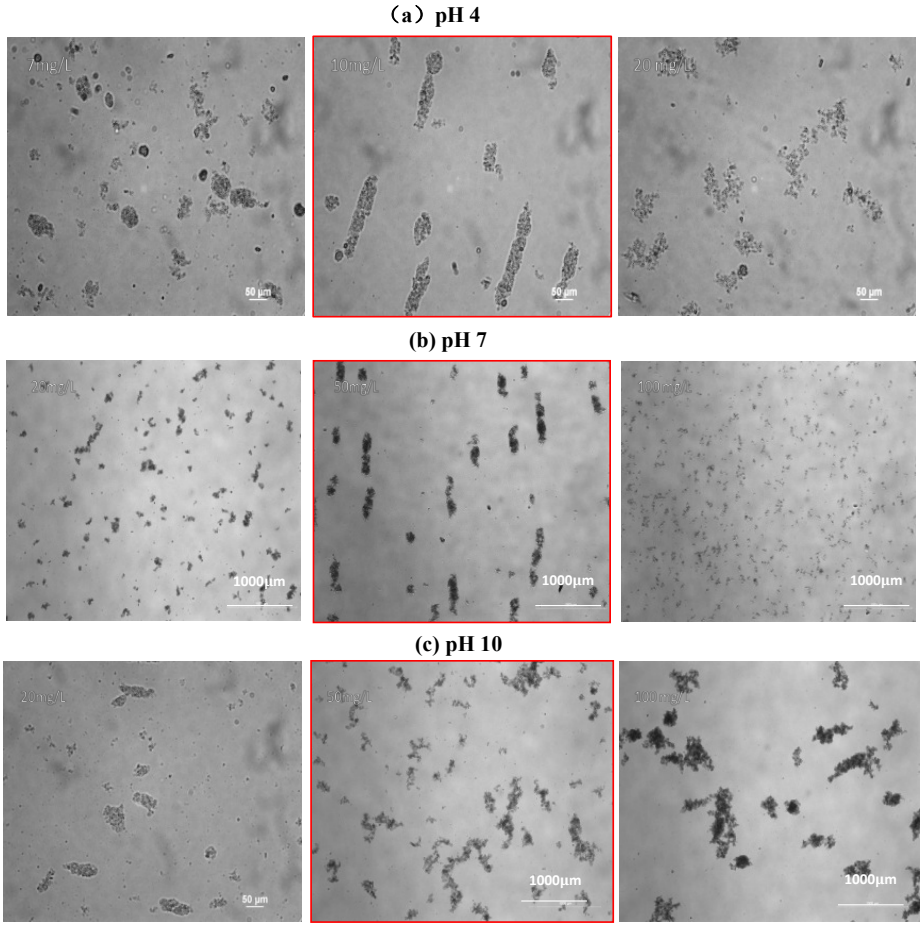

Figure 3.9 Microscopy image of floc under varied dosage of G-Chitosan a) pH 4, b) pH 7 and c) pH 10, OP has been marked out as red frame.

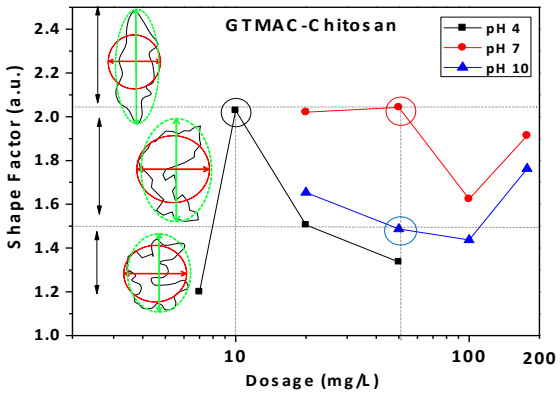

Figure 3.10 Shape factor with varied GTMAC-Chitosan dosage under pH 4, 7 and 10

From Figure 3.11, it can be seen that flocs from G-Chitosan/A-CNCs were verified to be more solid and spherical, particularly at the OD for all the pHs. The larger and darker floc images presented in the figure were expected to have a more densely packed structure. This closely aggregated packing was ascribed to the building up of cluster fragments constituting a spherical appearance. In the case of G-Chitosan/A-CNCs, the large increase in the mean particle size was also linked to the flocs having a compact and concrete structure, which was highly favorable for dewatering and sludge disposal.[194] The pH had a lesser effect on the flocculation behavior. However, the floc pattern observed in dosages both below and above the OD were found to be less smooth and discrete. The flocs of these particles/clusters appeared to be multibranched rather than one uniform piece, while the large spatial occupation was preserved. Further insights were extracted from the shape factor, which showed a comparatively smaller range of values within the same flocculation dosage. This corresponded with the floc images, showing the integrated packing pattern of floc that yielded an F value that approached unity. The lower F value established that the incorporation of CNCs into the flocculants could optimize the floc shape. By taking advantage of their high aspect ratio, the enhanced collision facilitated the formation of uniform flocs and reduced interior void entrapment. The smallest F value occurred at the OD for pH 7 and 10, where the floc structure was more compact as observed from the large and dark segments. However, the F value was found to maximize at the OD for pH 4, which was thought to be caused by sufficient charge present within the floc due to the protonation of primary amine groups, which resulted in a more irregular shape.[192]

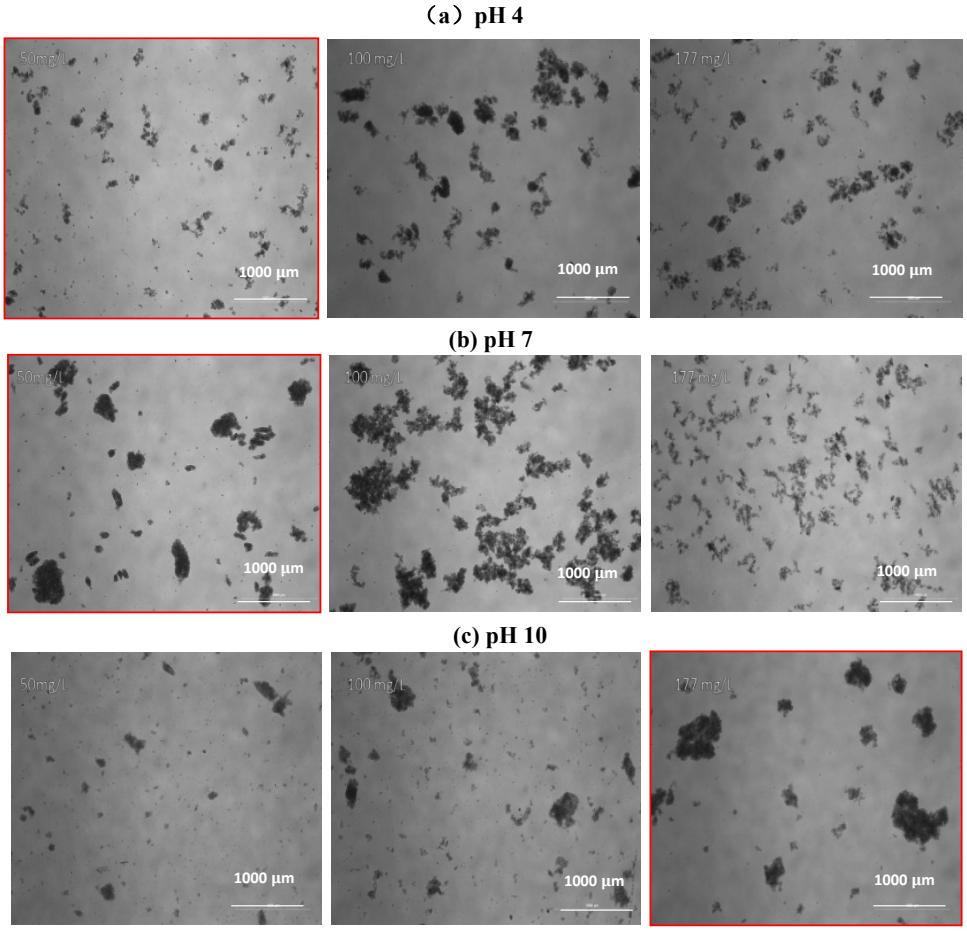

Figure 3.11 Microscopy image of floc under varied dosage of G-Chitosan/A-CNCs a) pH 4, b) pH 7 and c) pH 10, OP has been marked out as red frame.

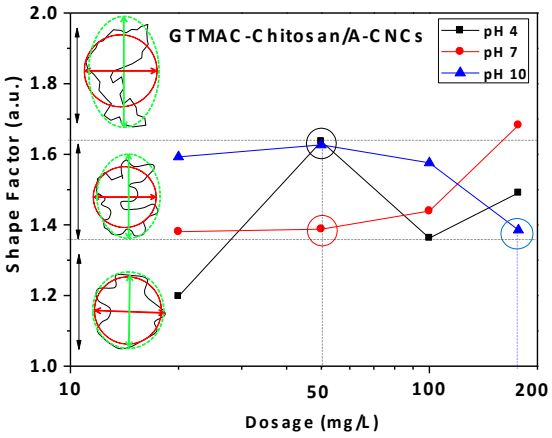

Figure 3.12 Shape factor with varied G-Chitosan/A-CNCs dosage under pH 4, 7 and 10.

A more common approach to determine the floc structure is using the fractal dimension, which relates the change of the longest dimension with the change of the area. By plotting the longest dimension of the floc "*l*" against the change of its area "A", we can determine D_2, which gives an insight into the two-dimensional floc shape.[195] This statistical value will only be valid if enough samples were analyzed. It is commonly accepted that densely packed aggregates have a higher fractal dimension, while branched and loosely bound structures have a lower value. As shown in Table 3.1, the D_2 values were generally smaller for G-Chitosan compared to G-Chitosan/A-CNCs, and the uniform floc of the latter was proven to also have a more compact and concrete internal distribution.

The lowest value observed at pH 4 of G-Chitosan was attributed to steric repulsion that yielded a looser floc structures. However, the best performance occurred at pH 7, where the flocs were elongated and created less voids. This was more obviously in the case of G-Chitosan/A-CNCs at all pHs, where the D_2 values have been significantly improved. This implied that the incorporation of nanoparticles in the flocculants contributed to the secondary association, and the agglomeration was expected to be more favorable to closely packing, moreover, this feature was maintained throughout all the pH levels.

Table 3.1 The optimal dosages and corresponding dimension fractal parameter D_2

Flocculants		G-Chitosan	G-Chitosan/A-CNCs
pH=4	$Dosage_{optimal}$ (mg/L)	10	50
	F & D_2	2.02 &1.67	1.63 &1.79
	Equivalent floc size(μm)	72	307
pH=7	$Dosage_{optimal}$ (mg/L)	50	50
	F & D_2	2.04 &1.78	1.39 &1.85
	Equivalent floc size(μm)	141	717
pH=10	$Dosage_{optimal}$ (mg/L)	50	177
	F & D_2	1.49 &1.72	1.38 &1.87
	Equivalent floc size(μm)	332	436

a. Dosage $_{optimal}$ is the optimal dosage where the lowest residual turbidity percentage occurs
b. F was measured by L/D, ratio between longest dimension and mean diameter
c. D_2 was measured by l A and determined from the slope of the log-log plot A and l

3.4 Comparison between GTMAC-Chitosan and G-Chitosan/A-CNCs

In the G-Chitosan polymer flocculants, the interactions predominantly occurred between positive charged sites and negative charged clay particles, and the OD dosage for each pH was comparatively lower than the G-Chitosan/A-CNCs. However, just as with common polymer flocculants, restabilization over the overdosing range is obvious through the evidence of deterioration of residual turbidity as well as reversed floc charge properties. In the G-Chitosan/A-CNCs, flocculation occurred between the chitosan and bentonite clay, where the Schiff base linkages partially consumed the primary amine groups, and electrostatic interactions occurred between the residual amine groups and negatively charged clays. Since CNCs constituted the majority of the flocculant's mass, a higher dosage was required to achieve optimal residual turbidity. But, the lowest residual turbidity was maintained, even though surface charge of floc became positive, but restabilization was not observed.

Under acidic conditions, high charge density of polymer produced a more intensive secondary polymer structures and stronger electrostatic interactions caused the polymer to adopt a "flat" layer on the clay particle surface. Thus charge neutralization dominated the flocculation pathways, and this effect was gradually substituted by a bridging effect with increasing pH. For the G-Chitosan/A-CNC system, charge attraction between two oppositely charge moieties occurred first, and the floc formation occured between the substrate of CNCs particle, where the polymer structure playing a minor role. Incorporating CNCs into flocculants was desirable to produce much larger floc sizes, which also possessed more effective morphology.

Flocs containing GTMAC-Chitosan that were found to be elliptical or linear in shape under acidic condition were caused by the strong repulsion between aggregates. In contrast, G-Chitosan/A-CNCs produced near-spherical aggregates, which bore clear evidence of the incorporation of CNCs that caused the floc to have a more integral interior distribution with a shape factor closer to unity (Table 3.1). A more thorough analysis can be drawn from the floc morphology through factual dimension of possible floc packing density. It was further supported by the high value of D_2 in Table 3.1, where the uniform floc was found to also have a more compact and concrete internal distribution. The integrated floc structure, indicated by higher floc density, was more favorable for floc settling velocity, dewatering ability and sequential phase separation.[196] The impact of the polymer charge density and polymer chain structure was diminished in this novel polymer/nanoparticle composite.

3.5 Conclusions

Modified Chitosan and G-Chitosan/A-CNCs flocculants were successfully prepared, and the characteristic FTIR peaks of each flocculants confirmed that GTMAC moieties were functionalized on Chitosan, as well as G-Chitosan being incorporated onto aldehyde CNCs. Flocculation experiments of both systems at three pH levels were conducted to systematically investigate the flocculation behavior, which included the flocculation efficiency in terms of residual turbidity, floc surface properties, as well as further insights into the floc morphology.

It was clear that both flocculants operated with different flocculation mechanisms. Charge density from the functional groups governed the electrostatic interaction between polymer flocculants with clay particle as well the adsorption fashion of polymer chain, which changed from charge neutralization to polymer bridging to patch attachment over the whole pH range. However, the impact of the polymer was less significant when it was associated with CNCs particle as a novel flocculants, with the significant change of flocculation mechanism. The charge attraction initially connected clay particles with the flocculants, though it is through the high aspect ratio and hydrophobic stiff backbone of CNCs where most of the particle collision occurred.

Differences between the samples were established by quantitatively measuring a large number of well-dispersed flocs selected without bias from microscopic images. Large and statistically significant differences in the average aggregate size were found between G-Chitosan and G-Chitosan/A-CNCs. As expected, the larger mean sizes from the G-C/A-CNCs flocs were proven to be uniform and spherical. On the other hand, flocs originated from polymers themselves showed

more irregular shapes and more elliptical outlines. The packing density was further investigated by the D_2 value and polymer/CNCs flocculants were proven to have a more compact and concrete floc structure. However, these optimized desirable floc features were achieved by sacrificing higher amount of flocculants dosage that can be attributed to the incorporation of CNCs.

Chapter 4. Conclusions and Recommendation for Future Studies

4.1 Conclusions

The major topic of my research focuses on the development of bio-flocculants from modified CNCs to remove suspended organic and inorganic colloids. In the treatment of latex particle, three different types of amine-containing monomers i.e. N-N-(dimethyl amino) ethyl methacrylate (DMA), 4-vinylpyridine (4VP), 2-hydroxy-3-chloro propylamine were utilized to graft from CNCs surface to produce cationic flocculants. Flocculation experiments were carried out to investigate the influence of various parameters, such as pH, mixing ratio between amine group and carboxylic acid group on latex particle, and amine types on the flocculation performance. It was observed that the change in the conformation of amine groups and polymer structure determined the flocculation efficiency and the flocculation mechanism pathway. At pH=4, charge neutralization was suggested for amine-g-CNCs and PDMA-g-CNCs and re-stabilization occurred at higher mixing ratio. Bridging effect was more obvious for P4VP that produced relatively large flocs.

For the inorganic clay, grafted onto approach was used to incorporate chitosan onto CNC surface to produce G-chitosan/A-CNC. In addition to exploring the profiles of the flocculation efficiency, floc surface properties, further insights on the floc morphology was advanced. The larger aggregates from G-Chitosan/A-CNCs were uniform and spherical like and yielded a more compact floc structure as suggested by D_2 value. The modified CNCs were proven to be an effective bio-flocculants.

4.2 Recommendation for future studies

In recently years, more development has been advanced on hybrid material both in the coagulants and flocculants. One disadvantage of polymer flocculants is that they often undergo coiling and loose their secondary structure in high ionic strength medium and alkali condition. The common focuses are dedicated to produce coagulants/flocculants with higher molecular weights, extended polymer structure that are more favorable for bridging effects and enhanced tolerability to high ionic strength. Another approach is to optimize flocs properties, which included larger and denser flocs, fast settling velocity, compact and integrated flocs interior structure, good dewatering ability and low sludge volume.

Novel polymer system such as the dual polymer, polymer/microparticle system has been proposed to optimizing the flocculation process. The pH and thermo-responsive characters are included in the dual system, for instance, amphoteric polymer can retain the constructive polymer structure over a wide pH range.[197] The main idea of incorporating thermal responsive moieties such as poly (N-isopropyl acrylamide) (PNIPAM) and poly(N-vinylcaprolactam) (PNVCL), into flocculants structure is that we can tune the flocculation and sedimentation above its lowest critical solution temperature (LCST) of the polymer flocculants, where a further increase in the temperature above the LSCT polymers will transform the soluble polymer chains into hydrophobic moieties that yield a more compact sediment, and low water content in the flocs, as presented in Scheme 5.1.

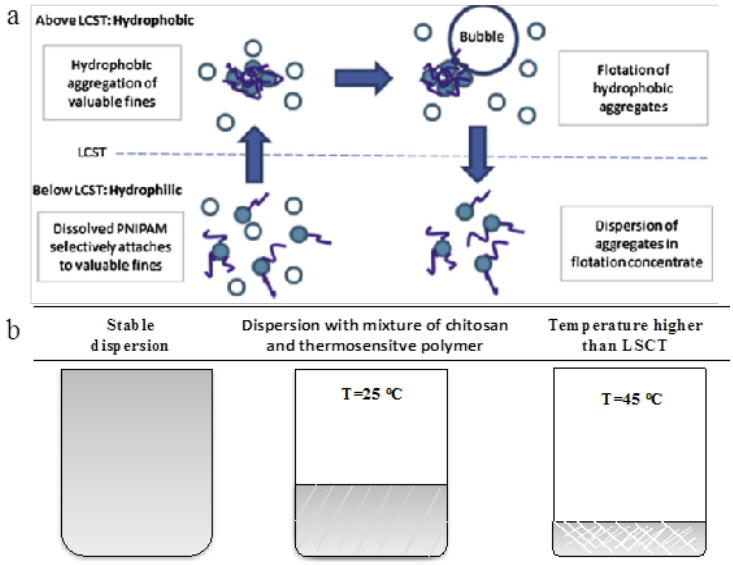

Scheme 5.1 (a) PNIPAM-AA as a flocculants, collector and dispersant at both side of LCST with minerals. (b) chitosan with Poly(N-vinylcaprolactam) (PNVCL) flocculation, sediment before and after LCST.

We have demonstrated modified CNCs as an effective flocculants for colloidal flocculation; this polymer/nanoparticle is a promising candidate to optimize flocs properties. Incorporating thermal responsive polymer onto CNCs could add to this bio-flocculants with new feature for the application in consolidating the sediment and enhancing dewatering capability.

Reference

[1] G. Bitton, *Wastewater Microbiology*, John Wiley & Sons, **2005**.

[2] R. L. Wershaw, P. J. Burcar, M. C. Goldberg, *Environ. Sci. Technol.* **1969**, *3*, 271.

[3] E. D. Caldas, R. Coelho, L. Souza, S. C. Silva, *Bull. Environ. Contam. Toxicol.* **1999**, *62*, 199.

[4] R. Ramalho, *Introduction to Wastewater Treatment Processes*, Elsevier, **2012**.

[5] A. Feigin, I. Ravina, J. Shalhevet, *Irrigation with Treated Sewage Effluent: Management for Environmental Protection*, Springer Science & Business Media, **2012**.

[6] J. Carrera, T. Vicent, J. Lafuente, *Process Biochem.* **2004**, *39*, 2035.

[7] C. F. Forster, *Wastewater Treatment and Technology*, Thomas Telford, **2003**.

[8] M. Henze, *Wastewater Treatment: Biological and Chemical Processes*, Springer Science & Business Media, **2002**.

[9] W. W. Eckenfelder, W. W. Eckenfelder, D. L. Ford, A. J. Englande, *Industrial Water Quality*, McGraw-Hill Professional, **2008**.

[10] A. Joss, S. Zabczynski, A. Göbel, B. Hoffmann, D. Löffler, C. S. McArdell, T. A. Ternes, A. Thomsen, H. Siegrist, *Water Res.* **2006**, *40*, 1686.

[11] J. P. Bell, M. Tsezos, *J. (Water Pollut. Control Fed.* **1987**, 191.

[12] P. J. Purcell, *Water Environ. J.* **2005**, *19*, 404.

[13] J. Bratby, *Engl. Uplands* **1980**.

[14] X. Guo, Z. Wu, M. He, *Water Res.* **2009**, *43*, 4327.

[15] A. Rosi'nska, L. D\kabrowska, *Desalin. Water Treat.* **2013**, *51*, 1657.

[16] X. Liu, X. M. Li, Q. Yang, X. Yue, T. T. Shen, W. Zheng, K. Luo, Y. H. Sun, G. M. Zeng, *Chem. Eng. J.* **2012**, *200-202*, 39.

[17] N. S. M. Zin, H. A. Aziz, M. N. Adlan, A. Ariffin, M. S. Yusoff, I. Dahlan, *Desalin. Water Treat.* **2014**, *3994*, 1.

[18] D. Vandamme, I. Foubert, K. Muylaert, *Trends Biotechnol.* **2013**, *31*, 233.

[19] F. Roselet, D. Vandamme, M. Roselet, K. Muylaert, P. C. Abreu, *Algal Res.* **2015**, *10*, 183.

[20] N. Sanyano, P. Chetpattananondh, S. Chongkhong, *Bioresour. Technol.* **2013**, *147*, 471.

[21] E.-S. Salama, J. R. Kim, M.-K. Ji, D.-W. Cho, R. a. I. Abou-Shanab, A. N. Kabra, B.-H. Jeon, *Bioresour. Technol.* **2015**, *186*, 232.

[22] Y. Y. Lau, Y. S. Wong, T. T. Teng, N. Morad, M. Rafatullah, S. A. Ong, *Chem. Eng. J.* **2014**, *246*, 383.

[23] J. Wei, B. Gao, Q. Yue, Y. Wang, *Chem. Eng. J.* **2009**, *151*, 176.

[24] A. Szyguła, E. Guibal, M. A. Palacín, M. Ruiz, A. M. Sastre, *J. Environ. Manage.* **2009**, *90*, 2979.

[25] K. L. Yeap, T. T. Teng, B. T. Poh, N. Morad, K. E. Lee, *Chem. Eng. J.* **2014**, *243*, 305.

[26] K. L. Yeap, T. T. Teng, B. T. Poh, N. Morad, K. E. Lee, *Chem. Eng. J.* **2014**, *243*, 305.

[27] E. Guibal, J. Roussy, *React. Funct. Polym.* **2007**, *67*, 33.

[28] Y. Al-Ani, Y. Li, *J. Taiwan Inst. Chem. Eng.* **2012**, *43*, 942.

[29] P. A. Moussas, A. I. Zouboulis, *Water Res.* **2009**, *43*, 3511.

[30] V. Pallier, G. Feuillade-Cathalifaud, B. Serpaud, J. C. Bollinger, *J. Colloid Interface Sci.* **2010**, *342*, 26.

[31] M.-Q. Yan, D.-S. Wang, B.-Y. Shi, Q.-S. Wei, J.-H. Qu, H.-X. Tang, *J. Environ. Sci. (China)* **2007**, *19*, 271.

[32] H. Zemmouri, M. Drouiche, A. Sayeh, H. Lounici, N. Mameri, *Procedia Eng.* **2012**, *33*, 254.

[33] M. Guida, M. Mattei, C. Della Rocca, G. Melluso, S. Meriç, *Desalination* **2007**, *211*, 113.

[34] R. Bergamasco, C. Bouchard, F. V. da Silva, M. H. M. Reis, M. R. Fagundes-Klen, *Desalination* **2009**, *245*, 205.

[35] M. I. Aguilar, J. Sáez, M. Lloréns, a. Soler, J. F. Ortuño, *Water Res.* **2002**, *36*, 2910.

[36] O. S. Amuda, A. Alade, *Desalination* **2006**, *196*, 22.

[37] R. W. O'Brien, L. R. White, *J. Chem. Soc. Faraday Trans. 2 Mol. Chem. Phys.* **1978**, *74*, 1607.

[38] J. Gregory, V. Dupont, *Water Sci. Technol.* **2001**, *44*, 231.

[39] F. Sher, A. Malik, H. Liu, *J. Environ. Chem. Eng.* **2013**, *1*, 684.

[40] J. M. Ebeling, P. L. Sibrell, S. R. Ogden, S. T. Summerfelt, *Aquac. Eng.* **2003**, *29*, 23.

[41] J.-Q. Jiang, *Curr. Opin. Chem. Eng.* **2015**, *8*, 36.

[42] G. P. 't Lam, M. H. Vermuë, G. Olivieri, L. a M. van den Broek, M. J. Barbosa, M. H. M. Eppink, R. H. Wijffels, D. M. M. Kleinegris, *Bioresour. Technol.* **2014**, *169*, 804.

[43] J. Addai-Mensah, *Powder Technol.* **2007**, *179*, 73.

[44] F. AlMubaddal, K. AlRumaihi, a. Ajbar, *J. Hazard. Mater.* **2009**, *161*, 431.

[45] E. Arinaitwe, M. Pawlik, *Int. J. Miner. Process.* **2009**, *91*, 50.

[46] L. Besra, D. K. Sengupta, S. K. Roy, *Int. J. Miner. Process.* **2006**, *78*, 101.

[47] J. F. Buyel, R. Fischer, *J. Biotechnol.* **2015**, *195*, 37.

[48] J. H. Choi, W. S. Shin, S. H. Lee, D. J. Joo, J. D. Lee, S. J. Choi, *Environ. Technol.* **2001**, *22*, 1025.

[49] M. T. O. de Velásquez, O. Manero, J. Cardoso, G. Martínez, *Environ. Technol.* **1998**, *19*, 323.

[50] S. Haydar, J. A. Aziz, *J. Hazard. Mater.* **2009**, *168*, 1035.

[51] S. H. Lee, W. S. Shin, M. C. Shin, S. J. Choi, L. S. Park, *Environ. Technol.* **2001**, *22*, 653.

[52] W. S. Ng, R. Sonsie, E. Forbes, G. V. Franks, *Miner. Eng.* **2015**, *77*, 64.

[53] M. Radoiu, *J. Hazard. Mater.* **2004**, *106*, 27.

[54] M. G. El Meligy, S. El Rafie, K. M. Abu-Zied, *Desalination* **2005**, *173*, 33.

[55] a. Hebeish, a. Higazy, a. El-Shafei, S. Sharaf, *Carbohydr. Polym.* **2010**, *79*, 60.

[56] K. H. M. Kan, J. Li, K. Wijesekera, E. D. Cranston, *Biomacromolecules* **2013**, *14*, 3130.

[57] Y. Lu, Y. Shang, X. Huang, A. Chen, Z. Yang, Y. Jiang, J. Cai, W. Gu, X. Qian, H. Yang, R. Cheng, **2011**, 7141.

[58] S. Schwarz, S. M. Ponce-Vargas, A. Licea-Claverie, C. Steinbach, *Colloids Surfaces A Physicochem. Eng. Asp.* **2012**, *413*, 7.

[59] B. R. Nayak, R. P. Singh, *J. Appl. Polym. Sci.* **2001**, *81*, 1776.

[60] S. Pal, A. Pal, *Polym. Bull.* **2012**, *69*, 545.

[61] S. Pal, G. Sen, S. Ghosh, R. P. Singh, *Carbohydr. Polym.* **2012**, *87*, 336.

[62] R. P. S. S.K. Rath, *Colloids Surfaces A Physicochem. Eng. Asp.* **1998**, *139*, 129.

[63] Y. Wei, X. Dong, A. Ding, D. Xie, *J. Taiwan Inst. Chem. Eng.* **2015**, *000*, 1.

[64] F. M. Pang, P. Kumar, T. T. Teng, A. K. Mohd Omar, K. L. Wasewar, *J. Taiwan Inst. Chem. Eng.* **2011**, *42*, 809.

[65] W. Xu, B. Gao, Y. Wang, Q. Zhang, Q. Yue, *Chem. Eng. J.* **2012**, *181-182*, 407.

[66] W. Sun, J. Long, Z. Xu, J. H. Masliyah, *Langmuir* **2008**, *24*, 14015.

[67] W. . Yang, J. . Qian, Z. . Shen, *J. Colloid Interface Sci.* **2004**, *273*, 400.

[68] W. Y. Yang, J. W. Qian, Z. Q. Shen, *J. Colloid Interface Sci.* **2004**, *273*, 400.

[69] J. Gregory, V. Dupont, *Water Sci. Technol.* **2001**, *44*, 231.

[70] R. Das, S. Ghorai, S. Pal, *Chem. Eng. J.* **2013**, *229*, 144.

[71] Y. Song, W. Gan, Q. Li, Y. Guo, J. Zhou, L. Zhang, *Carbohydr. Polym.* **2011**, *86*, 171.

[72] D. Vandamme, S. Eyley, G. Van den Mooter, K. Muylaert, W. Thielemans, *Bioresour. Technol.* **2015**, *194*, 270.

[73] M. Ashmore, J. Hearn, *Langmuir* **2000**, *16*, 4906.

[74] M. C. Garcia, A. A. Szogi, M. B. Vanotti, J. P. Chastain, P. D. Millner, *Bioresour. Technol.* **2009**, *100*, 5417.

[75] J. Roussy, M. Van Vooren, B. a. Dempsey, E. Guibal, *Water Res.* **2005**, *39*, 3247.

[76] Z. Yang, H. Li, H. Yan, H. Wu, H. Yang, Q. Wu, H. Li, A. Li, R. Cheng, *J. Hazard. Mater.* **2014**, *276*, 480.

[77] Z. Yang, Y. Shang, Y. Lu, Y. Chen, X. Huang, A. Chen, Y. Jiang, W. Gu, X. Qian, H. Yang, R. Cheng, *Chem. Eng. J.* **2011**, *172*, 287.

[78] D. Zeng, J. Wu, J. F. Kennedy, *Carbohydr. Polym.* **2008**, *71*, 135.

[79] M. Khalil, A. Aly, *Starch-Stärke* **2001**, *53*, 84.

[80] H. Kolya, 557–564. http://doi.org/10.1016/j.ijbiomac.2013.09.018Tridib Tripathy, Kolya, H., & Tripathy, T. (2013). Preparation, investigation of metal ion removal and flocculation performances of grafted hydroxyethyl starch. International Journal of Biological Macromolecules, 62, *Int. J. Biol. Macromol.* **2013**, *62*, 557.

[81] K. Kumar, P. Adhikary, N. C. Karmakar, S. Gupta, R. P. Singh, S. Krishnamoorthi, *Carbohydr. Polym.* **2015**, *127*, 275.

[82] S. Pal, D. Mal, R. P. Singh, *Carbohydr. Polym.* **2005**, *59*, 417.

[83] J. Duan, J. Gregory, *Adv. Colloid Interface Sci.* **2003**, *100-102*, 475.

[84] H. Xu, R. Jiao, F. Xiao, D. Wang, *Colloids Surfaces A Physicochem. Eng. Asp.* **2014**, *446*, 139.

[85] K. E. Lee, N. Morad, T. T. Teng, B. T. Poh, *Chem. Eng. J.* **2012**, *203*, 370.

[86] B. . Gao, Q. . Yue, B. . Wang, Y. . Chu, *Colloids Surfaces A Physicochem. Eng. Asp.* **2003**, *229*, 121.

[87] L. Cai, Q. H. X. Tian, **2010**, 7.

[88] K. E. Lee, T. T. Teng, N. Morad, B. T. Poh, M. Mahalingam, *Desalination* **2011**, *266*, 108.

[89] H.-L. Wang, J.-Y. Cui, W.-F. Jiang, *Mater. Chem. Phys.* **2011**, *130*, 993.

[90] K. E. Lee, T. T. Teng, N. Morad, B. T. Poh, Y. F. Hong, *Sep. Purif. Technol.* **2010**, *75*, 346.

[91] K. Gopi, S. Balaji, B. Muthuvelan, *Iran. J. Energy Environ.* **2014**, *5*, 94.

[92] Y. Wang, B. Y. Gao, Q. Y. Yue, J. C. Wei, W. Z. Zhou, *Water Pract. Technol.* **2006**, *1*, DOI 10.2166/WPT.2006048.

[93] K. E. Lee, I. Khan, N. Morad, T. T. Teng, B. T. Poh, *J. Dispers. Sci. Technol.* **2011**, *33*, 1284.

[94] L. M. Conaway, **1999**.

[95] M. F. Chong, K. P. Lee, H. J. Chieng, I. I. S. B. Ramli, *Water Res.* **2009**, *43*, 3326.

[96] T. F. Yen, **1975**.

[97] Y. Inagaki, S. Kiuchi, *J. Mater. Cycles Waste Manag.* **2001**, *3*, 14.

[98] S. Haydar, J. A. Aziz, *J. Hazard. Mater.* **2009**, *168*, 1035.

[99] K. L. Morrissey, C. He, M. H. Wong, X. Zhao, R. Z. Chapman, S. L. Bender, W. D. Prevatt, M. P. Stoykovich, *Biotechnol. Bioeng.* **2015**, *112*, 74.

[100] M. R. Granados, F. G. Acien, C. Gomez, J. M. Fernandez-Sevilla, E. Molina Grima, *Bioresour. Technol.* **2012**, *118*, 102.

[101] Q. Y. Yue, B. Y. Gao, Y. Wang, H. Zhang, X. Sun, S. G. Wang, R. R. Gu, *J. Hazard. Mater.* **2008**, *152*, 221.

[102] C. S. Lee, J. Robinson, M. F. Chong, *Process Saf. Environ. Prot.* **2014**, *92*, 489.

[103] J. W. Qian, X. J. Xiang, W. Y. Yang, M. Wang, B. Q. Zheng, **2004**, *40*, 1699.

[104] W. Sun, G. Zhang, L. Pan, H. Li, A. Shi, *Int. J. Polym. Sci.* **2013**, *2013*, DOI 10.1155/2013/397027.

[105] Z. Jiang, J. Zhu, *ASIAN J. Chem.* **2014**, *26*, 629.

[106] A. Rabiee, A. Ershad-Langroudi, M. E. Zeynali, *Rev. Chem. Eng.* **2015**, *31*, 239.

[107] D. Jancula, E. Marsalkova, B. Marsalek, *Aquac. Int.* **2011**, *19*, 1207.

[108] S. Wang, C. Liu, Q. Li, *WATER Res.* **2013**, *47*, 4538.

[109] B. Tian, X. Ge, G. Pan, Z. Luan, *DESALINATION* **2007**, *208*, 134.

[110] Z. Abdollahi, M. Frounchi, S. Dadbin, *J. Ind. Eng. Chem.* **2011**, *17*, 580.

[111] Y. Zheng, A. Wang, *J. Chem. Eng. Data* **2010**, *55*, 3494.

[112] A. Ubowska, T. Spychaj, *POLIMERY* **2010**, *55*, 299.

[113] I. Cengiz, E. Sabah, S. Ozgen, H. Akyildiz, *J. Appl. Polym. Sci.* **2009**, *112*, 1258.

[114] E. Sabah, C. Aciksoz, **2012**, *48*, 555.

[115] P. Scott, P. Sciences, **n.d.**

[116] Y. D. Yan, S. M. Glover, G. J. Jameson, S. Biggs, *Int. J. Miner. Process.* **2004**, *73*, 161.

[117] R. Gaudreault, M. A. Whitehead, T. G. M. Van De Ven, **n.d.**, 155.

[118] P. Mpofu, J. Addai-Mensah, J. Ralston, *Miner. Eng.* **2004**, *17*, 411.

[119] C. Negro, E. Fuente, A. Blanco, J. Tijero, *AIChE J.* **2005**, *51*, 1022.

[120] M. Polyacrylamide, **1994**, *Polyacryla*, 805.

[121] E. Sabah, Z. E. Erkan, *FUEL* **2006**, *85*, 350.

[122] T. G. M. Van De Ven, M. A. Qasaimeh, J. Paris, *Colloids Surfaces A Physicochem. Eng. Asp.* **2004**, *248*, 151.

[123] C. Guo, L. Zhou, J. Lv, *Polym. Polym. Compos.* **2013**, *21*, 449.

[124] G. Petzold, A. Nebel, H. M. Buchhammer, K. Lunkwitz, *COLLOID Polym. Sci.* **1998**, *276*, 125.

[125] D. Dihang, P. Aimar, J. Kayem, S. N. Koungou, *Chem. Eng. Process. Process Intensif.* **2008**, *47*, 1509.

[126] K. B. Musabekov, N. K. Tusupbaev, S. E. Kudaibergenov, *Macromol. Chem. Phys.* **1998**, *199*, 401.

[127] C. S. Lee, M. F. Chong, J. Robinson, E. Binner, **2014**.

[128] F. Renault, B. Sancey, P. M. Badot, G. Crini, *Eur. Polym. J.* **2009**, *45*, 1337.

[129] J. P. Wang, Y. Z. Chen, S. J. Yuan, G. P. Sheng, H. Q. Yu, *Water Res.* **2009**, *43*, 5267.

[130] R. Miranda, R. Nicu, I. Latour, M. Lupei, E. Bobu, A. Blanco, *Chem. Eng. J.* **2013**, *231*, 304.

[131] J. Roussy, M. Van Vooren, E. Guibal, *J. Appl. Polym. Sci.* **2005**, *98*, 2070.

[132] Z. LI, G. WANG, T. WANG, Y. MENG, *J. Saf. Environ.* **2008**, *3*, 16.

[133] Y.-C. Chung, Y.-H. Li, C.-C. Chen, *J. Environ. Sci. Heal.* **2005**, *40*, 1775.

[134] F. Gassara, C. Antzak, C. M. Ajila, S. J. Sarma, S. K. Brar, M. Verma, *J. Food Eng.* **2015**, *166*, 80.

[135] E. S. Beach, M. J. Eckelman, Z. Cui, L. Brentner, J. B. Zimmerman, *Bioresour. Technol.* **2012**, *121*, 445.

[136] G. Chen, L. Zhao, Y. Qi, Y.-L. Cui, *J. Nanomater.* **2014**, *2014*, 1.

[137] Y. Xu, S. Purton, F. Baganz, *Bioresour. Technol.* **2013**, *129*, 296.

[138] N. Rashid, S. U. Rehman, J. I. Han, *Process Biochem.* **2013**, *48*, 1107.

[139] M. Rinaudo, *Prog. Polym. Sci.* **2006**, *31*, 603.

[140] Z. Yang, B. Yuan, X. Huang, J. Zhou, J. Cai, H. Yang, A. Li, R. Cheng, *Water Res.* **2012**, *46*, 107.

[141] B. Yuan, Y. Shang, Y. Lu, Z. Qin, Y. Jiang, A. Chen, X. Qian, G. Wang, H. Yang, R. Cheng, *J. Appl. Polym. Sci.* **2010**, *117*, 1876.

[142] Y. Lu, Y. Shang, X. Huang, A. Chen, Z. Yang, Y. Jiang, J. Cai, W. Gu, X. Qian, H. Yang, R. Cheng, *Ind. Eng. Chem. Res.* **2011**, *50*, 7141.

[143] Z. Yang, Y. Shang, X. Huang, Y. Chen, Y. Lu, A. Chen, Y. Jiang, W. Gu, X. Qian, H. Yang, R. Cheng, *J. Environ. Sci. (China)* **2012**, *24*, 1378.

[144] A. Hebeish, A. Higazy, A. El-Shafei, *STARCH-STARKE* **2006**, *58*, 401.

[145] D. Zhao, J. Xu, L. Wang, J. Du, K. Dong, C. Wang, X. Liu, *J. Appl. Polym. Sci.* **2012**, *125*, E299.

[146] M. Mihai, E. S. Dragan, *Colloids Surfaces A Physicochem. Eng. Asp.* **2009**, *346*, 39.

[147] S. J. Eichhorn, A. Dufresne, M. Aranguren, N. E. Marcovich, J. R. Capadona, S. J. Rowan, C. Weder, W. Thielemans, M. Roman, S. Renneckar, W. Gindl, S. Veigel, J. Keckes, H. Yano, K. Abe, M. Nogi, a. N. Nakagaito, A. Mangalam, J. Simonsen, a. S. Benight, A. Bismarck, L. a. Berglund, T. Peijs, *Review: Current International Research into Cellulose Nanofibres and Nanocomposites*, **2010**.

[148] P. J. Quinlan, A. Tanvir, K. C. Tam, *Carbohydr. Polym.* **2015**, *133*, 80.

[149] H. Zhu, Y. Zhang, X. Yang, H. Liu, L. Shao, X. Zhang, J. Yao, *J. Hazard. Mater.* **2015**, *296*, 1.

[150] N. R. Mandre, D. Panigrahi, **1997**, *50*, 177.

[151] T. Suopajärvi, H. Liimatainen, O. Hormi, J. Niinimäki, *Chem. Eng. J.* **2013**, *231*, 59.

[152] R. Wu, L. Tian, W. Wang, X. Man, *J. Appl. Polym. Sci.* **2015**, *132*, n/a.

[153] U. J. Kim, S. Kuga, *Thermochim. Acta* **2001**, *369*, 79.

[154] J. Sirviö, A. Honka, H. Liimatainen, J. Niinimäki, O. Hormi, *Carbohydr. Polym.* **2011**, *86*, 266.

[155] S. Mishra, G. Usha Rani, G. Sen, *Carbohydr. Polym.* **2012**, *87*, 2255.

[156] H. Liu, X. Yang, Y. Zhang, H. Zhu, J. Yao, *Water Res.* **2014**, *59*, 165.

[157] H. Kono, R. Kusumoto, *React. Funct. Polym.* **2014**, *82*, 111.

[158] A. a. Aly, *Starch/Staerke* **2006**, *58*, 391.

[159] J.-P. Wang, S.-J. Yuan, Y. Wang, H.-Q. Yu, *Water Res.* **2013**, *47*, 2643.

[160] W. Jiraprasertkul, R. Nuisin, W. Jinsart, S. Kiatkamjornwong, *J. Appl. Polym. Sci.* **2006**, *102*, 2915.

[161] G. Sen, R. Kumar, S. Ghosh, S. Pal, *Carbohydr. Polym.* **2009**, *77*, 822.

[162] H. Li, T. Cai, B. Yuan, R. Li, H. Yang, A. Li, *Ind. Eng. Chem. Res.* **2015**, *54*, 59.

[163] Z. Yang, B. Yuan, H. Li, Y. Yang, H. Yang, A. Li, R. Cheng, *COLLOIDS SURFACES A-PHYSICOCHEMICAL Eng. Asp.* **2014**, *455*, 28.

[164] Z. Yang, H. Wu, B. Yuan, M. Huang, H. Yang, A. Li, J. Bai, R. Cheng, *Chem. Eng. J.* **2014**, *244*, 209.

[165] R. Rojas-Reyna, S. Schwarz, G. Heinrich, G. Petzold, S. Schütze, J. Bohrisch, *Carbohydr. Polym.* **2010**, *81*, 317.

[166] L. Ghimici, M. Nichifor, *Bioresour. Technol.* **2010**, *101*, 8549.

[167] P. Zugenmaier, *Crystalline Cellulose and Cellulose Derivatives*, **2008**.

[168] J. Tang, M. F. X. Lee, W. Zhang, B. Zhao, R. M. Berry, K. C. Tam, *Biomacromolecules* **2014**, *15*, 3052.

[169] E. Guibal, M. Van Vooren, B. a. Dempsey, J. Roussy, *Sep. Sci. Technol.* **2006**, *41*, 2487.

[170] J.-F. Gohy, S. Antoun, R. Jérôme, *Macromolecules* **2001**, *34*, 7435.

[171] A. L. Loeb, J. T. G. Overbeek, P. H. Wiersema, C. V King, *J. Electrochem. Soc.* **1961**, *108*, 269C.

[172] J. F. Tan, P. Ravi, H.-P. Too, T. A. Hatton, K. C. Tam, *Biomacromolecules* **2005**, *6*, 498.

[173] X. Sui, J. Yuan, M. Zhou, J. Zhang, H. Yang, W. Yuan, Y. Wei, C. Pan, *Biomacromolecules* **2008**, *9*, 2615.

[174] D. R. NAGHAMMAHMOODALJAMALI, *Int. J. Curr. Res. Chem. Pharma. Sci* **2014**, *1*, 121.

[175] M. K. Cyranski, *Chem. Rev.* **2005**, *105*, 3773.

[176] S. P. Akhlaghi, M. Zaman, N. Mohammed, C. Brinatti, R. Batmaz, R. Berry, W. Loh, K. C. Tam, *Carbohydr. Res.* **2015**, *409*, 48.

[177] E. a. López-Maldonado, M. T. Oropeza-Guzman, J. L. Jurado-Baizaval, a. Ochoa-Terán, *J. Hazard. Mater.* **2014**, *279*, 1.

[178] S. E. Kudaibergenov, S. E. Kudaibergenov, *Adv. Polym. Sci.* **1999**, *144*.

[179] J. Gregory, *Water Sci. Technol.* **1997**, *36*, 1.

[180] M. S. Nasser, A. E. James, **2006**, *51*, 10.

[181] P. Jarvis, B. Jefferson, S. A. Parsons, *Rev. Environ. Sci. Biotechnol.* **2005**, *4*, 1.

[182] J. Cho, J. Grant, M. Piquette-Miller, C. Allen, *Biomacromolecules* **2006**, *7*, 2845.

[183] G. F. Davidson, T. P. Nevell, *J. Text. Inst. Trans.* **1948**, *39*, T102.

[184] S.-P. Rwei, Y.-M. Chen, W.-Y. Lin, W.-Y. Chiang, *Mar. Drugs* **2014**, 5547.

[185] N. Drogat, R. Granet, V. Sol, A. Memmi, N. Saad, C. K. Koerkamp, P. Bressollier, P. Krausz, *J. Nanoparticle Res.* **2011**, *13*, 1557.

[186] E. Joussein, S. Petit, J. Churchman, B. Theng, D. Righi, B. Delvaux, *Clay Miner.* **2005**, *40*, 383.

[187] F. Annabi-Bergaya, M. I. Cruz, L. Gatineau, J. J. Fripiat, *Clay Miner.* **1979**, *14*, 249.

[188] Y.-H. Wang, W.-K. Siu, *Can. Geotech. J.* **2006**, *43*, 601.

[189] R. P. Singh, T. Tripathy, G. P. Karmakar, S. K. Rath, N. C. Karmakar, S. R. Pandey, K. Kannan, S. K. Jain, N. T. Lan, *Curr. Sci.* **2000**, *78*, 798.

[190] J. Li, S. Jiao, L. Zhong, J. Pan, Q. Ma, *Colloids Surfaces A Physicochem. Eng. Asp.* **2013**, *428*, 100.

[191] J. Li, X. Song, J. Pan, L. Zhong, S. Jiao, Q. Ma, *Int. J. Biol. Macromol.* **2013**, *62*, 4.

[192] S. Tang, J. Preece, C. McFarlane, Z. Zhang, *J. Colloid Interface Sci.* **2000**, *221*, 114.

[193] a. I. Medalia, F. a. Heckman, *Carbon N. Y.* **1969**, *7*, 567.

[194] P. S. Yen, L. C. Chen, C. Y. Chien, R. M. Wu, D. J. Lee, *Water Res.* **2002**, *36*, 539.

[195] F. Maggi, *J. Geophys. Res. Ocean.* **2007**, *112*, 1.

[196] J. Namer, J. J. Ganczarczyk, *Water Res.* **1993**, *27*, 1285.

[197] A. Rabiee, A. Ershad-Langroudi, H. Jamshidi, *Rev. Chem. Eng.* **2014**, *30*, 501.